博士論文

Synthesis, Structure Analysis and Antifungal Activities of Hypervalent Organobismuth(III) Compounds

（超原子価有機ビスマス(III)化合物の合成と構造解析および抗真菌活性）

平成 30 年 9 月

A. F. M. HAFIZUR RAHMAN

山口大学大学院医学系研究科

Contents

Chapter 1

INTRODUCTION

1.1. BISMUTH

Bismuth, Bi is a chemical element and 83rd element of the periodic table, a pentavalent post-transition metal and one of the pnictogens, chemically resembles its lighter homologs Arsenic and Antimony. The etymology is uncertain but possibly comes from Arabic *bi ismid*, meaning having the properties of Antimony [1] or the German word *Weiße Masse* or Wismuth ('white mass') translated in the mid-sixteenth century to new Latin *bisemutum* [2]. Bismuth was first shown to be a distinct element in 1753 by Claude Geoffroy the Younger. Although bismuth is usually obtained as a bi-product of mining and refining lead, copper, tin, silver, and gold but the largest deposits of bismuth are found in Bolivia. The free bismuth element is 86% as dense as lead and when freshly produced it is a brittle metal with a silvery white color but surface oxidation can give it a pink tinge [https://en.wikipedia.org/wiki/Bismuth].

Bismuth

In crystallography, bismuth shows the hexagonal crystal family which includes two crystal systems (hexagonal and trigonal) and two lattice systems (hexagonal and rhombohedral) [3].

Crystal system	Trigonal	Hexagonal	
Lattice system	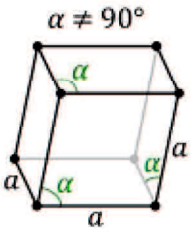 Rhombohedral	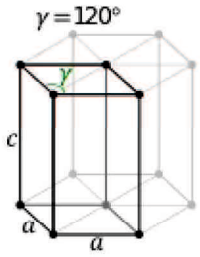 Hexagonal	
Example	 Dolomite	 Cinnabar	 Beryl

Bismuth metal is brittle and so is usually mixed with other metals, such as lead, tin, iron or cadmium to form low melting alloys which make it useful. These alloys with low melting points are used in automatic fire sprinkler systems, fire detectors and extinguishers, electric fuses and solders [4]. Bismuth has several uses in chemistry or medicine. Bismuth oxide (Bi_2O_3) is used as a yellow pigment in paints and cosmetics and bismuth oxychloride (BiOCl) is used to make a pigment, Bismuth white. Bismuth carbonate [$Bi_2(CO_3)_2$] is used to treat diarrhea and gastric ulcers. Bismuth subsalicylate, pink bismuth, brand name Pepto-Bismol is an antacid medication [5,6] used to treat temporary discomforts of the stomach and gastrointestinal tracts like diarrhea, indigestion, heartburn and nausea. Sodium bismuth tartrate was formerly used to treat syphilis [7,8]. As a derivative of salicylic acid, bismuth subsalicylate displays anti-inflammatory [9] and bactericidal action [10].

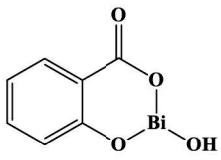

Bismuth subsalicylate

Industrially bismuth is considered as one of the less toxic heavy metals but there are some adverse effects of bismuth subsalicylate. It can cause a black tongue and black stools in some users of the drug, when it combines with trace amounts of sulfur in saliva and the colon to form bismuth sulfide [11]. Bismuth sulfide is a highly insoluble black salt, and the discoloration seen is temporary and harmless. Long-term use (longer than 6 weeks) may lead to accumulation and toxicity [12]. Some of the risks of salicylism can apply to the use of bismuth subsalicylate [13-15].

Children should not take medication with bismuth subsalicylate while recovering from influenza or chicken pox, as epidemiologic evidence points to an association between the use of salicylate-containing medications during certain viral infections and the onset of Reye's syndrome [16]. For the same reason, it is typically recommended that nursing mothers do not use medication containing bismuth subsalicylate because small amounts of the medication are excreted in human breast milk, and these pose a theoretical risk of Reye's syndrome to nursing children [17]. Salicylates are very toxic to cats, and thus bismuth subsalicylate should not be administered to cats [18]. The British National Formulary does not recommend bismuth containing antacids (unless chelated), cautioning that absorbed bismuth can be neurotoxic, causing encephalopathy, and that such antacids tend to be constipating [19].

1.2. LITHIATION and ZINCATION

Lithiation: The lithiation is a chemical reaction that forms a temporary C-Li bond as an intermediate. The C−Li bond is highly ionic because the electronegativity gap between the carbon atom and the lithium atom is very large. As the polar nature of the C−Li bond, organolithium reagents act as good nucleophiles and strong bases. As highly polarized C−Li bond, the carbon attracts most of the electron density in the bond and tends to form a carbanion [20]. In the synthetic chemistry the organolithium reagents are used as nucleophiles for the

carbolithiation reactions, carbonylation, S_N2 type reactions and as a strong base for deprotonation, initiator for polymerization, metalation, transmetalation, Li-halogen exchange reaction and enolate formation [21]. Organolithium reagents are very useful in organic synthesis, but the high reactivities in some cases lead to some unexpected side reactions and cause the productivity very low. To avoid such unexpected situations, if we use some less reactive organic reagents like Grignard reagents or organozinc reagents, we may get the better expected results.

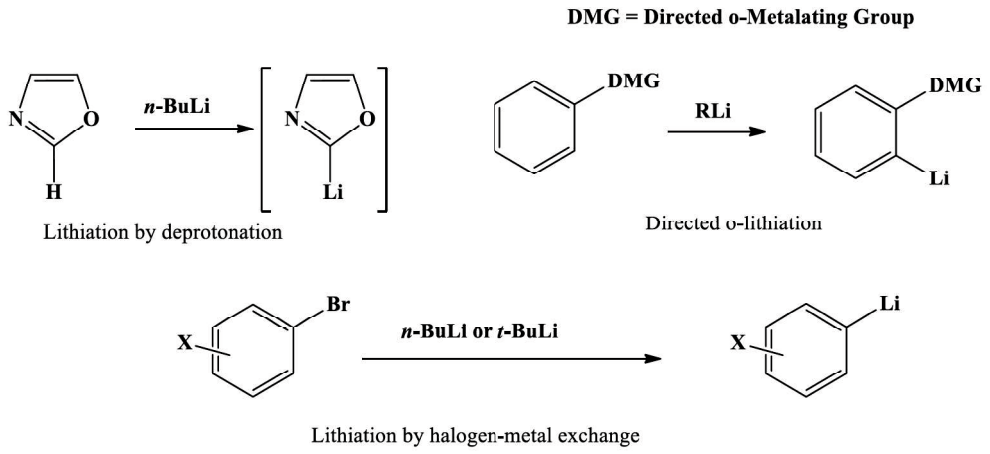

Various lithiation reactions

Zincation: A reaction that contains any metalation reaction involving zinc atom and forms at least one C−Zn bond is known as zincation. Zincation is very similar to Grignard reaction. Zincation is playing an important role in organic synthesis or organometallic chemistry. There are hundreds of organozinc reactions and their compounds already well-known. These reactions can be conducted in a one-pot procedure and established from last century and the range of zincation in organozinc chemistry is very wide.

Using TMP-zincate as a chemoselective base [22,23] directed ortho metalation (DoM) reaction of aromatic compounds by Gilman and Wittig [24] is the most effective method for the regioselective functionalization of aromatic compound [25]. Direct zincation of aromatics [26],

tropolone [27], benzyl methyl ether [28], benzamides and phenyl o-carbamate [29], catalytic zincation of aromatic and heteroaromatics [30] and selective zincation of unsymmetrical azobenzene [31] have been demonstrated in earlier years. Above all the zincation reactions were built by using Zn-reagent as a base and the reaction process required a longer reaction route.

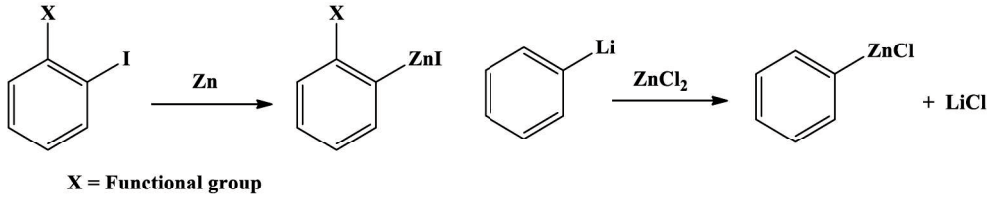

Zincation by metal insertion into carbon-halogen bond

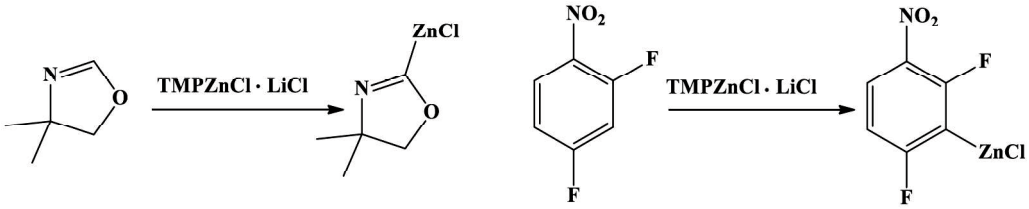

Directed zincation of aromatics and heteroaromatics by deprotonation

Various zincation reactions

Our interests are in achieving the hypervalent bond formation in phenyl-carbonyl compounds under mild conditions. Hence, the direct zincation of a C–I bond by metal insertion is suitable for such purpose because this method is very simple, economically friendly and mostly saves the time. Furthermore, to avoid the harsh conditions of using excess amount of BuLi, unnecessary temperature controlling and improvement of productivity is the main achiever of this method.

1.3. Log*P* and Clog*P*

The quality of chemical compounds that are able or shows the tendency to dissolve in fats, oils, lipids and non-polar solvents like hexane or toluene is known as lipophilicity and these non-polar solvents are themselves lipophilic. Lipophilic substances tend to dissolve in other lipophilic substances and hydrophilic components tend to dissolve in water and other hydrophilic substances. Lipophilic substances interact through the London dispersion force and they have a little to no capacity to form hydrogen bonds. Thus, the lipophilic and hydrophobic substances are immiscible or tend to be insoluble with each other because of the large o/w (octanol/water) partition coefficients.

The partition-coefficient (*P*) is the ratio of concentrations of substances in a mixture of two immiscible phases at the equilibrium condition and generally refers to the concentration ratio of the un-ionized species of substances. These ratios are therefore a measure of the difference in solubility of the compound in these two phases.

Log*P* is the logarithm of the partition coefficient of a molecule between an aqueous and lipophilic phase, usually *n*-octanol and water $\log(c_{octanol}/c_{water})$ which is a well-established measure of lipophilicity or hydrophilicity of the compounds. Low hydrophilicities and therefore high log*P* values cause poor absorption or permeation and *vice-versa* [32(a), (b)].

$$\log P_{oct/wat} = \log \left(\frac{[solute]^{un\text{-}ionized}_{octanol}}{[solute]^{un\text{-}ionized}_{water}} \right)$$

Clog*P* is the function in ChemDraw and is a calculated numeric value which depends on the structures of the chemical compounds.

1.4. DISSOCIATION ENERGY and ASSOCIATION ENERGY

Dissociation energy: [33] The dissociation energy is defined as that in a gaseous state, the enthalpy needed or how amount energy is required to break one mole of the bond to give the individual elements or to separate atoms. This is also known as bond dissociation energy or enthalpy. Dissociation energy differs from the bond energy or bond fusion energy/enthalpy. Bond dissociation energy is the energy of a single chemical bond while bond energy is the average of all the bond dissociation energies in a compound and the enthalpy of fusion of a substance is known as the enthalpy required to completely change the state of one mole of substance between solid and liquid states at constant pressure.

As for example, the bond dissociation energy to break up one mole of gaseous HCl into the gaseous hydrogen and chlorine atoms requires 432 kJ, that means the dissociation energy for H-Cl bond is +432 kJ mol^{-1}.

Association energy: [34] When one mole of crystalline or solid ionic substance is formed from its constituent ions in their gaseous state, the amount of change in enthalpy or energy released under the standard conditions by the system through the chemical reaction is known as association energy. That means that the energy that released in a chemical reaction by the system to stabilize or form a stable compound is the association energy or simply in a standard reaction condition the function of the association energy is in terms of reducing the temperature heat or pressure.

This association and association energies are closely related to the inhibition activities or antifungal activities. In our earlier works [35] we have explained about the relationship of the association or dissociation energies with inhibition zone. In this work we have proposed about the formation of an intermediate ate complex $[Ar_2BiXNu]^-$ shown in the plausible reaction pathway for bismuthane. This ate complex (path 2) is formed when the bismuthanes undergo

an addition at the bismuth atom with biomolecules and by using the methanethiolate anion as a model nucleophile (Nu^-), the association energies (enthalpies) have been calculated.

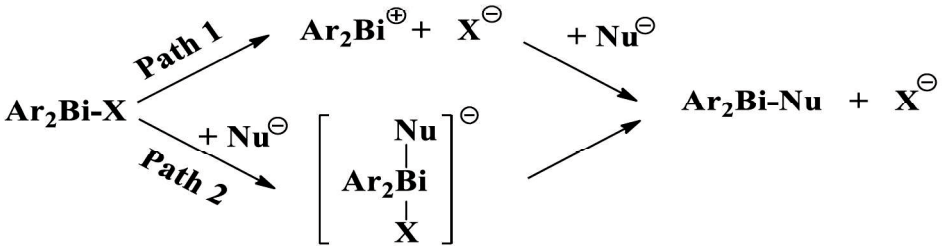

Plausible reaction pathway for bismuthanes

1.5. PHYSICAL PROPERTIES OF BISMUTH

Organobismuth chemistry is the chemistry of organometallic compounds containing a carbon to bismuth chemical bond. According to the scientists of organic chemistry, applications are rare even though bismuth and bismuth compounds are the least toxic among the heavy metals and are relatively cheap [36]. Bismuth is the element of group 15. Group 15 elements constitute the third column of the p-block of the periodic table and comprise the other elements nitrogen, phosphorus, arsenic and antimony. Considering the properties of group 15 elements, the ground state electronic configuration is $ns^2\ np^3$, which results the common oxidation states of +3 (III) and +5 (V) expect for the nitrogen, so the main bismuth oxidation states are Bi(III) and Bi(V). A list of some of the properties of the group 15 elements is shown in Table 1 [37].

Table 1. Some properties of group 15 elements.

Properties \ Elements	N	P	As	Sb	Bi
a) Properties of the isolated atom					
1) Atomic number	7	15	33	51	83
2) Atomic mass	14.007	30.97	74.92	121.75	208.98
3) 1st ionization energy (KJ/mol)	1402.3	1011.7	947.0	833.7	703.2
4) Electron affinity (KJ/mol)	-7	72.0	78.0	101.0	91.3
b) Properties of the bound atom					
1) Electronegativity					
i) Pauling scale	3.04	2.19	2.18	2.05	2.02
ii) Allred-Rochow scale	3.07	2.06	2.20	1.82	1.67
2) Atomic radius (Å)	0.71	0.93 (white)	1.25	1.82	1.55
3) Covalent radius (Å)	0.70	1.10	1.21	1.41	1.52
4) Van der Waals radius (Å)	1.54	1.90	2.00	2.20	2.40

In general, electronegativities are expected to decrease as the group is descended but according to the Pauling or Allred-Rochow scales, it should be noted that the electronegativities of phosphorus and arsenic are quite similar as are those of antimony and bismuth. Atomic properties closely related to electronegativity are ionization energy and electron affinity. The values of ionization energies decrease on descending the group. Another trend to note is that the atomic bound properties of this group is closely related to the various atomic radii such as covalent, ionic and van der Waals. From the above discussion, it is clear that the energy of a bond to carbon in this group decreases in the order P > As > Sb > Bi [38].

1.6. ORGANOBISMUTH COMPOUNDS

The slow development of organobismuth chemistry may be attributed to limited access to many compounds as well as the thermal or chemical instability of organobismuth compounds. About 45 years ago organobismuth compounds have come to be studied intensively and the uniqueness of bismuth in organic chemistry has become widely recognized, particularly increasing the attention for medicinal and electronic applications. The parent organobismuth heterocycles are bismole, bismabenzene, bismine, bismepin and bismocine.

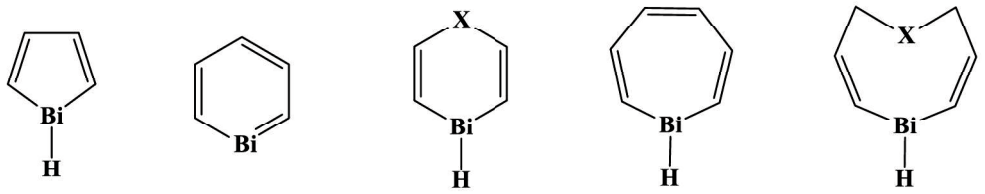

Bismuth heterocycles

The first reported use of bismuth in organic chemistry was in oxidation of alcohols by Challenger in 1934 [39]. Recent developments of organobismuth chemistry including our contributions are shown below.

a) Synthesis of optically active organobismuth compounds: [40]

Construction of optically active bismuth compounds was considered to be difficult due the lack of suitable methods for synthesis of these types of compounds. Recently, an optically pure bismuthane has been synthesized with exclusive stereoselectivity by using Bi-N intramolecular coordination and the planar chirality of ferrocene and characterized by X-ray structure analysis. This strategy may serve as a guide for asymmetric induction over other heteroatom centers.

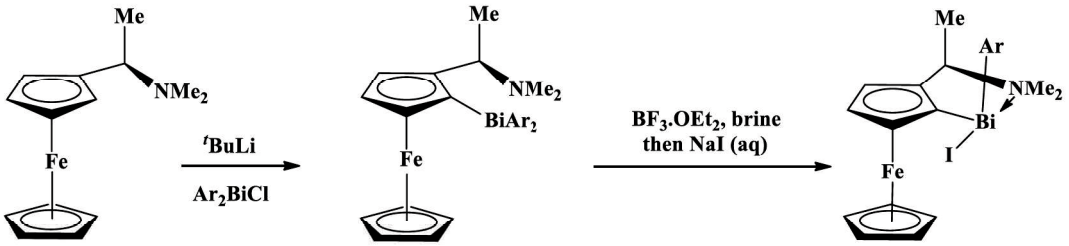

b) Synthesis of triarylbismuthanes bearing a π-acccpting cyano, ester or nitro group: [41]

Triarylbismuthanes bearing a π-accepting substituent are attractive for their crystalline states based on the donor–acceptor interactions. Introduction of an aryl group bearing a π-accepting substituent into the bismuth center was very limited. Very recently, a synthetic method for introducing such electron–withdrawing aryl group has been developed by using iodine–magnesium or iodine–lithium exchange reactions of the corresponding iodoarenes. This method has broad applicability for the synthesis of various mixed bismuthanes bearing π-accepting substituent.

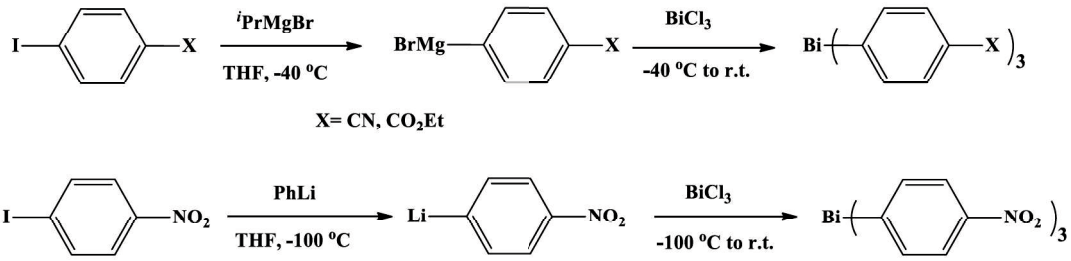

c) Synthesis of chiral bismuthanes: [42]

An aryl group present in asymmetrical triarylbismuthanes undergoes preferential displacement by another aryl group through transmetallation with an aryllithium reagent to give the corresponding chiral bismuthanes.

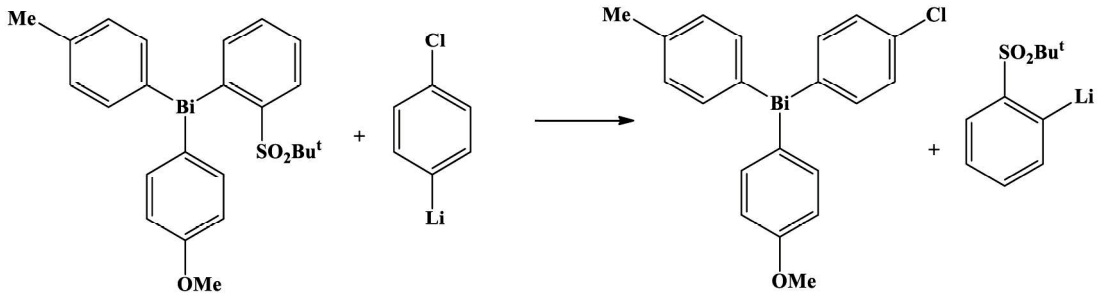

d) Halogenolysis and acidolysis of triarylbismuthanes: [43-46]

Triarylbismuthines can be converted to the corresponding diarylhalobismuthines in the presence of halogen such as iodine. On the other hand, Lewis acid and protic acid such as HBr cleave the Bi–C bond of triaryl bismuthanes to afford the corresponding halobismuthanes.

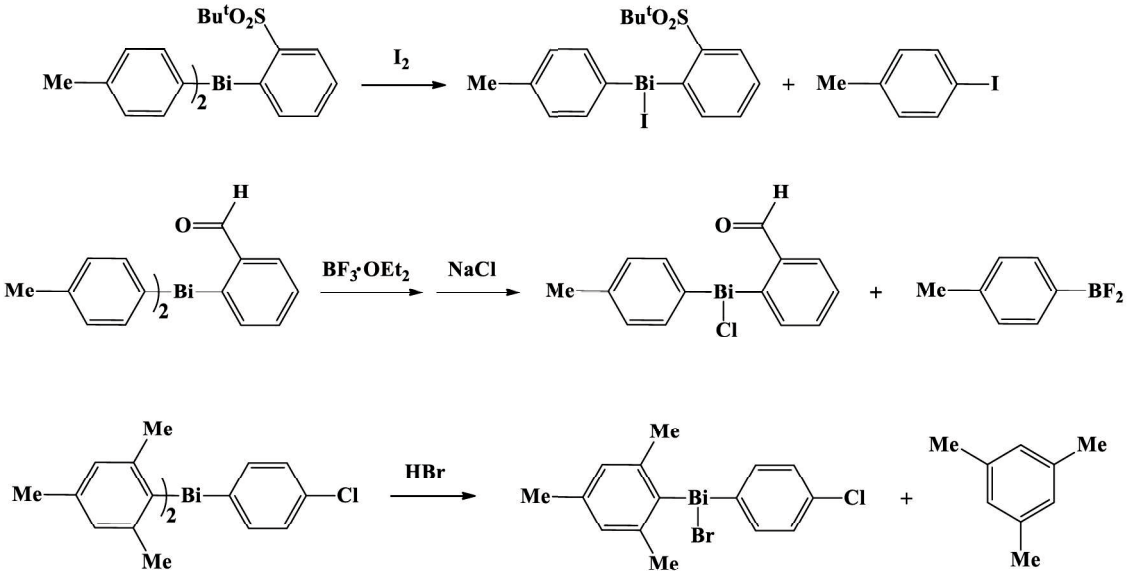

1.7. HYPERVALENT COMPOUNDS

A molecule that contains one or more main group elements evidently bearing more than eight electrons in their valence shells is known as a hypervalent molecule. This main group elements form one or more bonds, that would be counted by the octet rule or expanding octet. As the atoms contain more electrons in the outermost, the term is known as an 'expanded octet',

meaning that there are more than eight electrons around one atom. In 1969, this hypervalent molecules were first formally identified by Jeremy I. Musher, as molecules having central atoms of group 15–18 in any valence other than the lowest (*i.e.* 3, 2, 1, 0 for Groups 15, 16, 17, 18 respectively, based on the octet rule) [47]. In the first half of the twentieth century, the initial preparation of hypervalent organic molecules was carried out by Hermann Staudinger and Georg Wittig and they were able to show the challenge for extent valence theory and were success by preparing nitrogen and phosphorus-centered hypervalent molecules [48]. Hypervalent bismuth compound forms by the intramolecular coordination between the bismuth center and a heteroatom bearing a lone pair of electrons. A trivalent benzoxabismole bearing a hypervalent three-center-four-electron bond over the oxygen, bismuth and nitrogen atoms, *i.e.* a "10-Bi-4" type compound has been established by X-ray crystallography [49, 50].

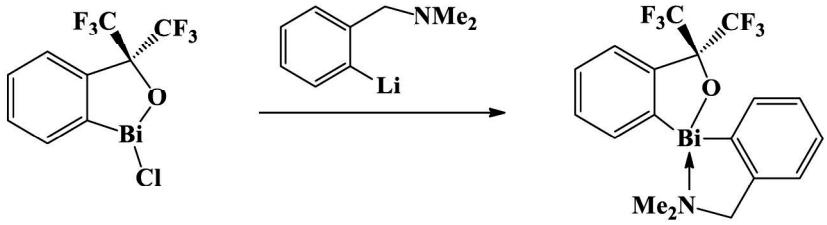

Unlike the analogous 10-Bi-4 benzoxabismole, a hexacoordinated benzoxabismole, 12-Bi-6 bearing similar coordination by the dimethyl amino group has also been characterized [51] and the electronegative oxygen and nitrogen atoms are in *cis* geometry.

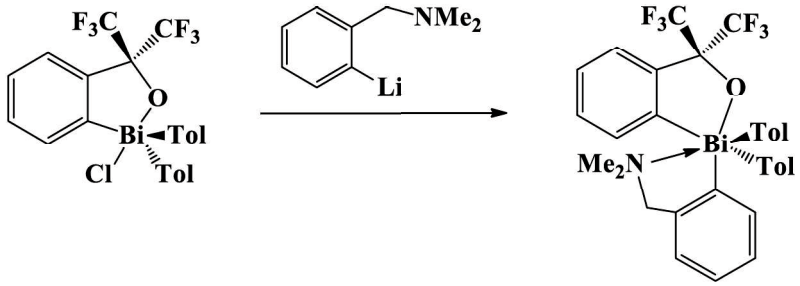

An example of hypervalent organobismuth compound by our contribution is shown below: [52] When a pentavalent bismuth dichloride is refluxed in dichloromethane, reductive elimination takes place smoothly to give chlorobismuthine and is considered to be facilitated by the transannular effect.

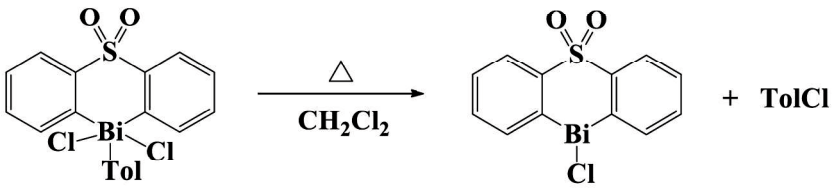

1.8. BIOLOGICALLY ACTIVE BISMUTH COMPOUNDS

In terms of its low level of toxicity and noncarcinogenic nature, bismuth is a unique element despite its heavy metal status. Traditionally, inorganic bismuth compounds have found widespread uses in medicine and veterinary practice. Various types of bismuth salts have been introduced as fungicides. They are also used as medicines for the treatment of gastrointestinal disorders due to their astringent, bacteriostatic, and disinfectant actions [53-55]. However, bismuth salts exhibit only modest antibacterial activity [56]. Bismuth salts have been extensively used as antimicrobial agents, and as cataloged by Briand and Burford [54]. Many bismuth-containing compounds with apparent chemical complexity exhibit therapeutic or antibacterial activity. Thus, bismuth compounds should be promising the great pharmaceutical agents. The structural studies of bismuth complexes indicate that Bi^{3+} has a variable coordination number, has an irregular coordination geometry, and is strongly acidic. In inorganic biochemistry bismuth also plays a vital role. Inhibition of (metallic) enzymes by bismuth may play an important role in the anti-bactericidal activity of bismuth containing drugs, and the inhibition is mainly ascribed to its binding to the key cysteine residue(s) within the enzyme. There are hundreds of uses of bismuth in inorganic chemistry but we treat here only

the biological activities of organobismuth compounds. The synthetic and antimicrobial studies of some of the organobismuth compounds by Kotani *et. al.* are shown below [57].

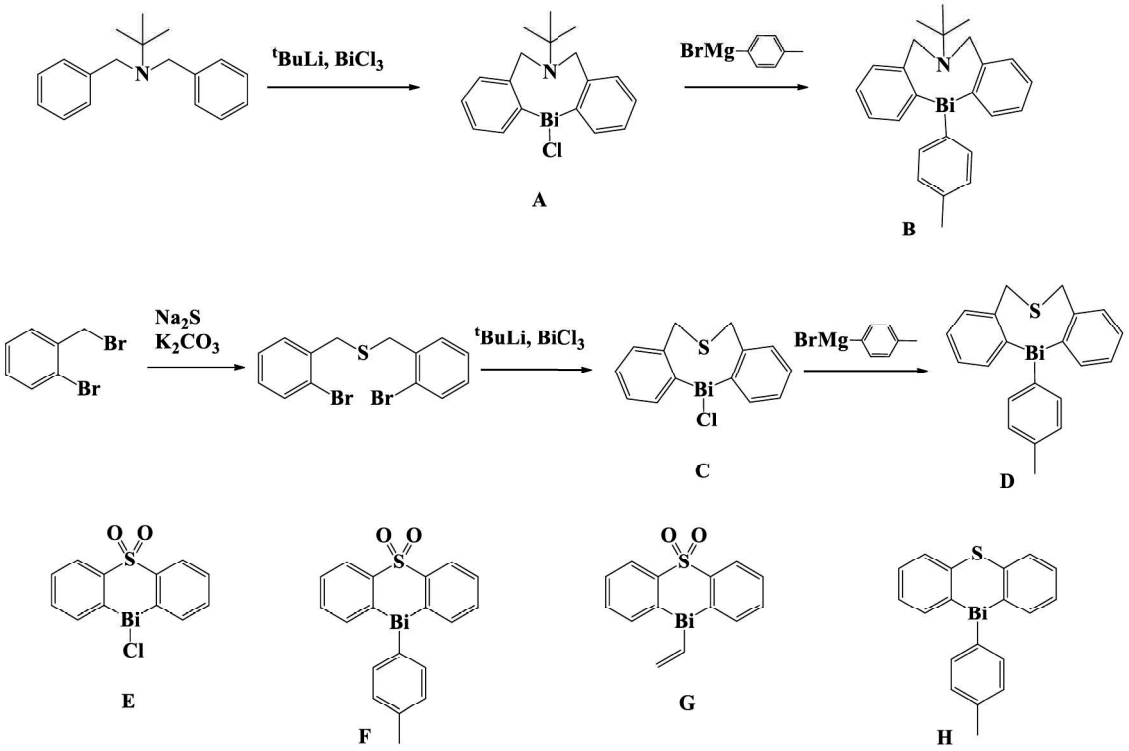

They have studied the biological activities of the above 8 compounds against five gram-positive and five gram-negative bacteria and noted that the bismuth compounds used in this study can be classified into three groups according to their antibacterial activities. Prominent activity was observed with compounds **A** to **C**, while moderate activity was exhibited by compounds **D, E** and **G**. Compounds **F** and **H** were weak in their actions. All eight-membered-ring compounds except compound **D** exhibited stronger antimicrobial activities than the six-membered compounds **E** to **H**. Compounds **A** and **C** were particularly active, where the bismuth and chlorine atoms can undergo transannular interaction with the nitrogen or sulfur atom via a hypervalent transition state.

1.9. RECENT REPORTS ON ANTIFUNGAL ORGANOBISMUTH COMPOUNDS

Bismuth is considered as a nontoxic and noncarcinogenic element. A number of bismuth compounds are lowly toxic and can be safely used in pharmaceuticals [37, 58]. Inorganic bismuth compounds have been extensively investigated as medicine for over two centuries [55], and some of them are widely used for clinic treatment of inflammatory diseases including gastric ulcer, gastritis and peptic ulcer [59]. Over the past decades, significant work has been devoted to the development of novel organobismuth drugs [60]. Some organobismuth complexes exhibited in vitro activities including those of antifungal and antiviral natures [61]. Recently a series of 8 membered hypervalent organobismuth compounds have been synthesized and their biological activities have been studied against a series of human cancer cell lines [62]. Among all the six compounds, compound **J** showed the strongest inhibitory effect on all cancer cell lines.

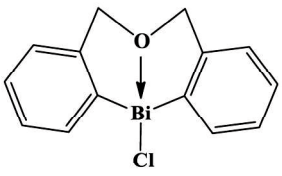

I

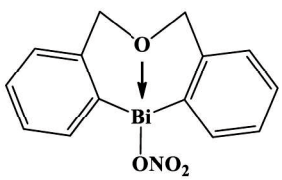

J

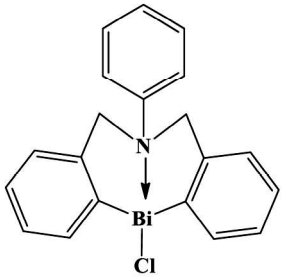

K

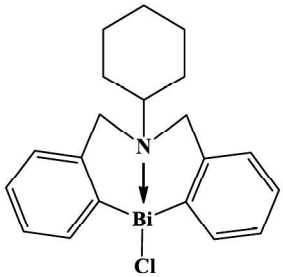

L

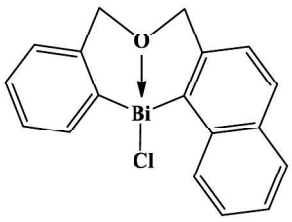

M

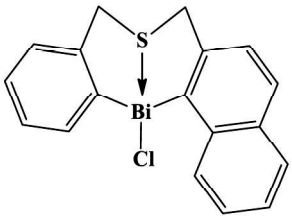

N

Our recent contributions of hypervalent organobismuth compounds to the study of synthesis and antifungal activities against ***S. cerevisiae*** have already been established as below.

a) **Organobismuth(III) compounds derived from alkyl aryl ketones:** [35]

Antifungal studies on hypervalent organobismuth compounds are not so ancient. Recently, we have reported the antifungal activity of hypervalent organobismuth(III) and (V) compounds against the yeast *Saccharomyces cerevisiae* [63, 64]. Compound **Q** ($R^1 = R^2 = H$) showed the higher activity but compounds **O, P** and **R** were less active compared **Q**.

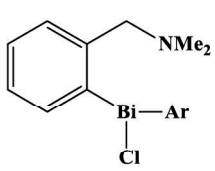

O

Ar = *p*-Tol
Ph

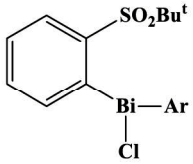

P

Ar = *p*-Tol
Ph

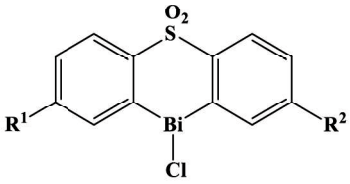

Q

$R^1 = R^2 = H$
$R^1 = R^2 = OH$

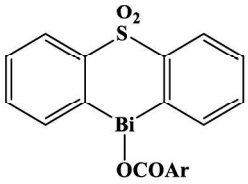

R

Ar = Ph
6-azulenyl

Modifying the system, we have designed a series of halobismuthanes **S-W** derived from alkyl aryl ketone by changing the alkyl and aryl groups of the ketone scaffold and attaching the aryl and halo groups to the bismuth atom. In this case halobismuthane **U** (Ar = 4-FC_6H_4) showed the highest activity compared to **Q**.

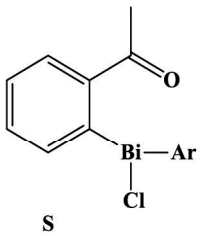

S

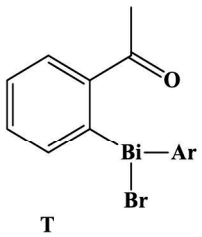

T

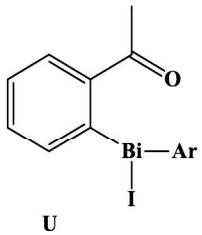

U

Ar = 4-$MeOC_6H_4$
4-MeC_6H_4 (Tol)
Ph
4-FC_6H_4
4-ClC_6H_4
2,4,6-$Me_3C_6H_2$

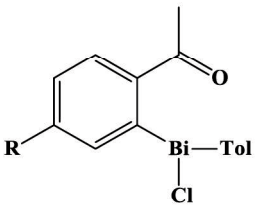

V

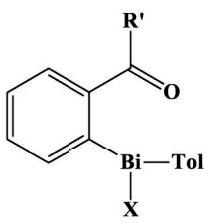

W

R = Me, *i*-Pr, MeO

R' = *n*-Pr, *n*-Bu, *i*-Pr
X = Cl, Br

b) Bismuth heterocycles based on diphenyl sulfone scaffold: [63]

In the diphenyl sulfone system, a series of organobismuth compounds have been synthesized and the antifungal activities of these bismuthanes have been studied against *S. cerevisiae* to know how the inhibition activity of **X(e)** is affected by either substitution on the diphenyl sulfone scaffold or by replacing of the chloro group attached to active bismuth center with an alternative electron withdrawing carboxylate group.

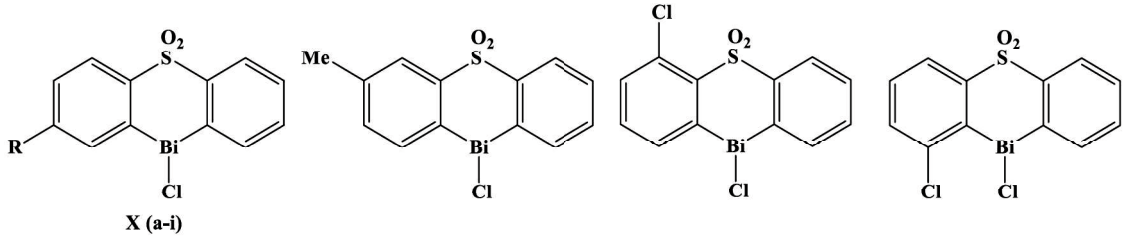

X (a-i)

R: a) = Me, b) = Ph, c) = OMe, d) = Cl, e) = H, f) = *t*-Bu, g) = CF_3, h) = F, i) = NMe_2

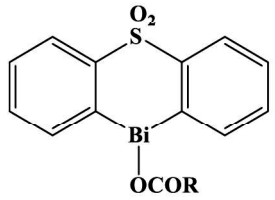

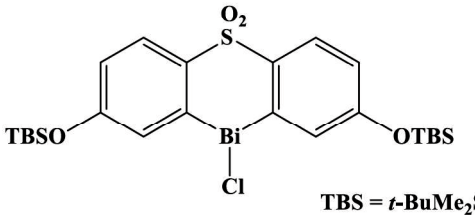

TBS = *t*-$BuMe_2Si$

R =

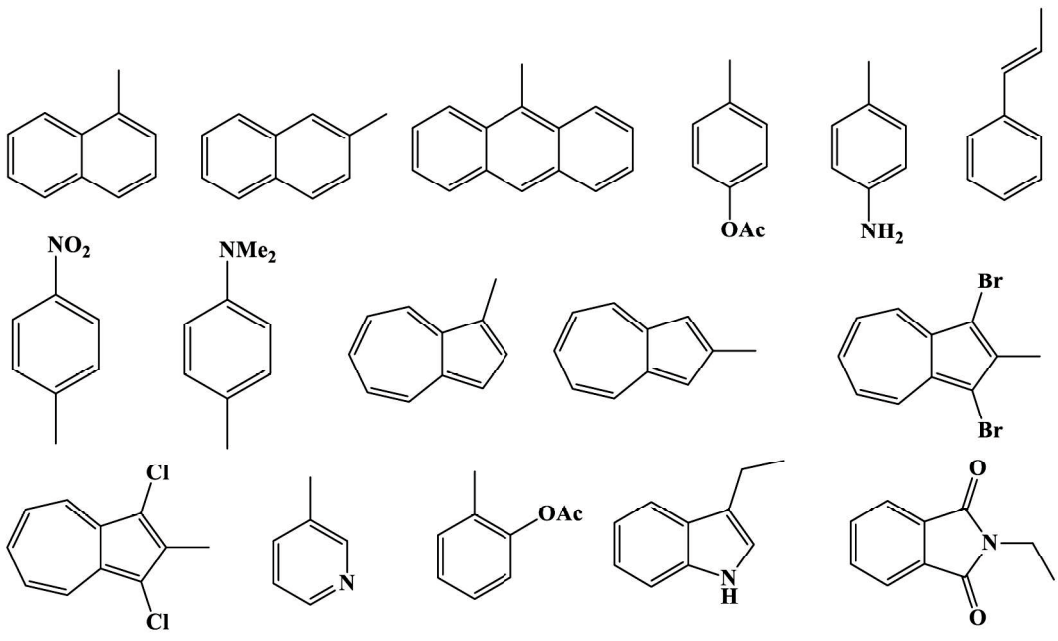

1.10. PURPOSES OF THIS RESEARCH WORK

The biological activity of bismuth compounds has attracted considerable interest. Although inorganic bismuth complexes have a long history in medicinal chemistry, the biological activity of organobismuth compounds is not well understood because their chemistry has only been established over the last two decades. In our laboratory, it has been revealed that the hypervalent organobismuth(III) compounds comprised of a diphenyl sulfone or acetophenone scaffold show high antifungal activities against the yeast *Saccharomyces cerevisiae*. Hence, the structural modification of these compounds is expected to give this class of compounds the activities that are comparable to or higher than the standard antifungal drug, nystatin. It is an important issue for us to develop the strategy to design more active antifungal organobismuth compounds. Our laboratory has already revealed that the Lewis acidy at the bismuth center is essential for generating the antifungal activity. On the other hand, we have found that several hypervalent organobismuth(III) compounds do not show any antifungal activities despite the presence of the Lewis acidity at the bismuth atom. These conflicting results led the author to consider not only the Lewis acidity but also other structural factors that affect their antifungal activities. Based on this idea, the author proposed the following two structural factors. Thus, one is ClogP, the commonly used measure of lipophilicity. The other is the association energy (enthalpy) in the exothermic association reaction that an intermediate ate complex $[Ar_2BiXNu]^-$ is formed by the bismuthanes Ar_2BiX undergoing addition at the bismuth atom with biomolecules Nu^- such as thiolate anion.

The purpose of this research work is to clarify the relationships between the ClogP and the antifungal activity and between the association energy and the antifungal activity. We studied the antifungal activities of iodobismuthanes derived from phenyl pyridinyl sulfones and o-carbonyl iodobenzenes from the viewpoint of these factors. Furthermore, a new synthetic

method for the hypervalent organobismuth compounds derived from o-carbonyl iodobenzenes was also developed by using organozinc reagents.

1.11. REFERENCES

[1] Bismuth. *Web Mineral. Retrieved on* 17 December **2011**. [https://en.wikipedia.org/wiki/Bismuth#cite_note-4].

[2] D. Harper, *"bismuth". Online Etymology Dictionary.* [https://en.wikipedia.org/wiki/Bismuth#cite_note-oet-5].

[3] J. Meija, T. B. Coplen, M. Berglund, W. A. Brand, P. de Blevre, M. Gronlng, N. E. Holden, J. Irrgeher, R. D. Loss, T. Walczyk, T. Prohaska, *Pure Appl. Chem.* **2016**, *88*, 265.

[4] J. Emsley, *Nature's Building Blocks: An A-Z Guide to the Elements*, Oxford University Press, New York, 2nd Edition, **2011**.

[5] S. Kean, *The Disappearing Spoon (and other true tales of madness, love, and the history of the world from the Periodic Table of Elements). New York/Boston: Back Bay Books,* **2011**, 158.

[6] C. R. Hammond, *The Elements, in Handbook of Chemistry and Physics (81st ed.). Boca Raton (FL, US): CRC press.* **2004**, 4.

[7] R. J. G. Parnell, *J. R. Soc. Med. (War section):* **1924**, *17*, 19.

[8] USA 1540117, G. Gustav, *"Manufacture of bismuth tartrates", Patent* [https://en.wikipedia.org/wiki/Bismuth#cite_note-65].

[9] A Madisch, A. Morgner, M. Stolte, S. Miehlke, *Expert Opin. Investig Drugs.* **2008**, *17*, 1829.

[10] H. L. DuPont, *Nat. Clin. Pract. Gastroenterol Hepatol.* **2005**, *2*, 191.

[11] *"Why does Pepto-Bismol sometimes darken the tongue/stool and how long does it last?". Pepto-Bismol FAQ. Pepto-Bismol.* [https://en.wikipedia.org/wiki/Bismuth_Subsalicylate#cite_note-4].

[12] S. L Gorbach, *Gastroenterology* **1990**, *99*, 863.

[13] *"Bismuth Subsalicylate". MedlinePlus. National Institutes of Health.* [https://en.wikipedia.org/wiki/Bismuth_Subsalicylate#cite_note-6].

[14] S. J Sainsbury, *West. J. Med.* **1991**, *155*, 637.

[15] M. A. Vernace, A. G Bellucci, B. M. Wilkes, *Am. J. Med.* **1994**, *97*, 308.

[16] *Aspirin or Salicylate-Containing Medications, reyessyndrome.org* [https://en.wikipedia.org/wiki/Bismuth_Subsalicylate#cite_note-9].

[17] *"Food-borne and Waterborne Illness - Breastfeeding – CDC".* cdc.gov. [https://en.wikipedia.org/wiki/Bismuth_Subsalicylate#cite_note-10].

[18] Carlson and Giffin, *Cat Owner's Home Veterinary Handbook*, page 390 [https://en.wikipedia.org/wiki/Bismuth_Subsalicylate#cite_note-11].

[19] *"1.1.1 Antacids and simeticone". Retrieved* **2018** [https://en.wikipedia.org/wiki/Bismuth_Subsalicylate#cite_note-12].

[20] J. Clayden, *Organolithiums: Selectivity for synthesis*, (*Tetrahedron Organic Chemistry Series*) **2002**, *23*.

[21] M. Schlosser, *Organometallics in Synthesis, A Manual* **2002** Second Edition

[22] Y. Kondo, M. Shilai, M. Uchiyama, T. Sakamoto, *J. Am. Chem. Soc.* **1999**, *121*, 3539.

[23] M. Uchiyama, Y. Matsumoto, S. Usui, Y. Hashimoto, K. Morokuma, *Angew. Chem. Int. Ed*. **2007**, *119*, 944.

[24] (a) H. Gilman, R. L. Bebb, *J. Am. Chem. Soc*. **1939**, *61*, 109. (b) G. Wittig, G. Fuhrman, *Chem. Ber*. **1940**, *73*, 1197. (c) H. Gilman, J. W. Morton, *J. Org. React.* **1954**, *8*, 258.

[25] (a) V. Snieckus, *Chem. Rev.* **1990**, *90*, 879. (b) H. W. Gschwend, H. R. Rodriguez, *Org. React. (N.Y.)* **1979**, *26*, 1.

[26] M. Mosrin, P. Knochel, *Org. Lett.* **2009**, *11*, 1837.

[27] D. Haas, D. Sustac-Roman, S. Schwarz, P. Knochel, *Org. Lett*. **2016**, *18*, 6380.

[28] L. Balloch, A. R. Kennedy, J. Klett, R. E. Mulvey, C. T. O'Hara, *Chem. Commun*. **2010**, *46*, 2319.

[29] L. Balloch, A. R. Kennedy, R. E. Mulvey, T. Rantanen, S. D. Robertson, V. Snieckus, *Organometallics* **2011**, *30*, 145.

[30] V. Guilarte, M. P. Castroviejo, E. Álvarez R. Sanz, *Beilstein J. Org. Chem.* **2011**, *7*, 1255.

[31] M. Ketels, K. Karaghiosoff, D. Trauner, P. Knochel, *Org. Lett*. **2017**, *19*, 1666.

[32] (a) A. J. Leo, *Chem. Rev.* **1993**, *93*, 1281. (b) A. J. Leo, C. Hansch, D. Eikins, *Chem. Rev.* **1971**, *71*, 525.

[33] *https://www.chemguid.co.uk/physical/energetics/bondenthalpies.html.*

[34] R. Sharma, A. Baid, L. S. Jayaram, *Ind. Eng. Chem. Res.* **1999**, *38*, 1057.

[35] T. Murafuji, M. Tomura, K. Ishiguro and I. Miyakawa, *Molecules* **2014**, *19*, 11077.

[36] Bismuth-Mediated Organic Reactions, T. Ollevier, *Ed. Topics in Current Chemistry, Springer Verlag, Berlin* **2012**, *311*, 277.

[37] N. C. Norman, "*Chemistry of Arsenic, Antimony and Bismuth*", *Thomson Science, 1st Edit.* **1998**, 1.

[38] C. Elschenbroich, A. Salzer *Organometallics: A Concise Introduction* (2nd Ed) **1992**, from Wiley-VCH: Weinheim. ISBN 3-527-28165-7

[39] F. Challenger and O. V. Richards, *J. Chem. Soc*. **1934**, 405.

[40] T. Murafuji, K. Satoh, Y. Sugihara, N. Azuma, *Organometallics* **1998**, *17*, 1711.

[41] T. Murafuji, K. Nishio, M. Nagasuc, A. Tanabe, M. Aono, Y. Sugihara, *Synthesis* **2000**, 1208.

[42] H. Suzuki and T. Murafuji, *J. Chem. Soc., Chem. Commun.* **1992**, 1143.

[43] H. Suzuki, T. Murafuji and N. Azuma, *J. Chem. Soc., Perkin Trans. 1* **1993**, 1169.

[44] T. Murafuji, T. Mutoh, K. Satoh, K. Tsunenari, N. Azuma, H. Suzuki, *Organometallics* **1995**, *14*, 3848.

[45] H. Suzuki, T. Murafuji, Y. Matano, N. Azuma, *J. Chem. Soc. Perkin Trans. 1* **1993**, 2969.

[46] T. Murafuji, N. Azuma, H. Suzuki, *Organometallics* **1995**, *14*, 1542.

[47] J. I. Musher, *Angew. Chem. Int. Ed.* **1969**, *8*, 54.

[48] K.-y. Akiba, *Chemistry of Hypervalent Compounds*. *New York: Wiley VCH*. ISBN 0-471-24019-2.

[49] Y. Yamamoto, X. Chen, K.-*y*. Akiba, *J. Am. Chem. Soc.* **1992**, *114*, 7906.

[50] Y. Yamamoto, X. Chen, S. Kojima, K. Ohdoi, M. Kitano, Y. Doi, K.-*y*. Akiba, *J. Am. Chem. Soc.* **1995**, *117*, 3922.

[51] Y. Yamamoto, K. Ohdoi, X. Chen, M. Kitano, K.-*y*. Akiba, *Organometallics* **1993**, *12*, 3297.

[52] H. Suzuki, T. Murafuji, N. Azuma, *J. Chem. Soc., Perkin Trans. 1* **1992**, 1593.

[53] D. W. Bierer, **1990**, *Bismuth subsalicylate: history, chemistry and safety. Rev. Infact.Dis. 12*(Suppl. 1): S3-S8.

[54] G. G. Briand and N. Burford, *Chem. Rev*. **1999**, *99*, 2601.

[55] H. Suzuki, N. Komatsu, T. Ogawa, T. Murafuji, T. Ikegami, Y. Matano, *Organobismuth Chemistry, Elsevier* **2001**.

[56] N. A. Cornick, M. Silva, S. L. Gorbach, **1990**, *In vitro antibacterial activity of bismuth subsalicylate. Rev. Infect. Dis. 12* (Suppl. 1): S9-S10.

[57] T. Kotani, D. Nagai, K. Asahi, H. Suzuki, F. Yamao, N. Kataoka, T. Yagura, *Antimicrob. Agents Chemother.* **2005**, *49*, 2729.

[58] G.I. Elliott, J.P. Konopelski, *Tetrahedron* **2001**, *57*, 5683.

[59] *E. R. Tiekink, Crit. Rev. Oncol. Hematol.* **2002**, *42*, 217.

[60] P.C. Andrews, M. Busse, G.B. Deacon, R.L. Ferrero, P.C. Junk, K.K. Huynh, I. Kumar, J.G. MacLellan, *Dalton Trans*. **2010**, *39*, 9633.

[61] K. Iuchi, Y. Hatano, T. Yagura, *Biochem. Pharmacol*. **2008**, *76*, 974.

[62] Y.P. Liu, J. Lei, L. Tang, Y. Peng, C.T. Au, Y, Chen, S.F. Yin, *Eur. J. Med. Chem.* **2017**, *139*, 826.

[63] (a) T. Murafuji, K. Kitagawa, D. Yoshimatsu, K. Kondo, K. Ishiguro, R. Tsunashima, I. Miyakawa, Y. Mikata, *Eur. J. Med. Chem.* **2013**, *63*, 531. (b) T. Murafuji, Y. Fujiwara, D. Yoshimatsu, I. Miyakawa, K. Migita, Y. Mikata, *Eur. J. Med. Chem.* **2011**, *46*, 519.

[64] T. Muafuji, Y. Miyoshi, M. Ishibashi, A. F. M. M. Rahman, Y. Sugihara, I. Miyakawa, H. Uno, *J. Inorg. Biochem.* **2004**, *98*, 547.

Chapter 2

SYNTHESIS AND ANTIFUNGAL ACTIVITIES OF PYRIDINE BIOISOSTERES OF A BISMUTH HETEROCYCLE DERIVED FROM DIPHENYL SULFONE

Abstract – Heterocyclic iodobismuthanes **7–9** [IBi(C_6H_4-2-$SO_2C_5H_3N$-1′-)] derived from phenyl pyridinyl sulfones were synthesized. Their antifungal activities against the yeast *Saccharomyces cerevisiae* were compared with those of halobismuthanes [XBi(RC_6H_3-2-$SO_2C_6H_4$-1′-)] (**1**: X=Cl; **2**: X=I, R=H) derived from diphenyl sulfone derivatives to determine how the bioisosteric replacement of the benzene ring in **2** with the pyridine ring in **7–9** affects their activities. The antifungal activities of **7–9** were higher or comparable to those of **1** and **2**. The DFT calculations suggested that the generation of the antifungal activity of the bismuthanes was well understood by the nucleophilic addition of methanethiolate anion as a model biomolecule at the bismuth atom to give an intermediate ate complex.

INTRODUCTION

Bismuth is a heavy metal that is less toxic to human in comparison to the metals surrounding it in the periodic table.[1–3] This factor makes it possible to use bismuth compounds as drugs in the treatment of gastrointestinal disorders,[1] a red light-excitable photosensitizer in cells,[2] and biocompatible catalysts for ring opening polymerization.[3] Biologically active bismuth compounds have been the subject of considerable interest due to their medicinal utility.[4–13] We have reported the synthesis and antifungal activity against the yeast *Saccharomyces cerevisiae* of bismuth heterocycles **1–3** (Scheme 1 and Table 2).[14–16]

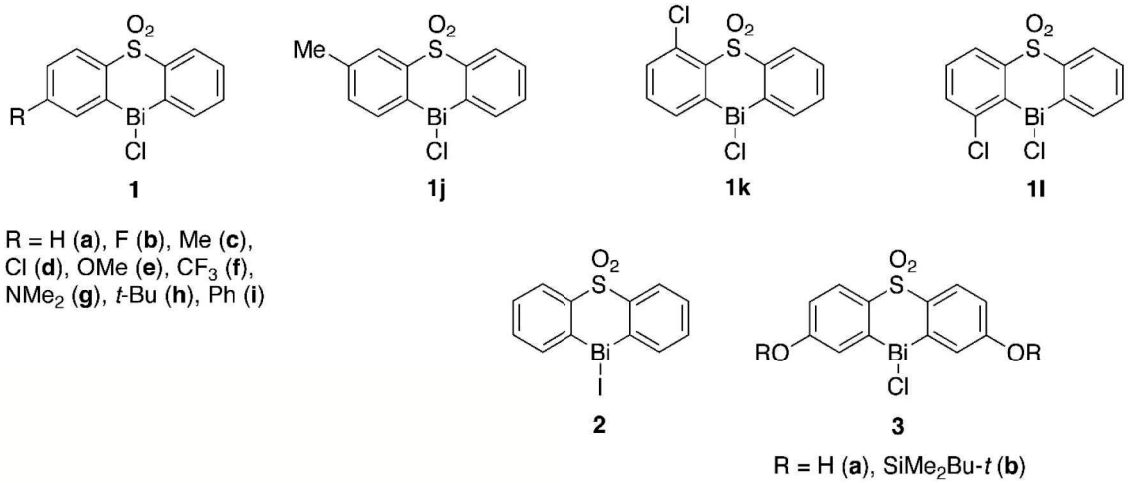

Scheme 1. Molecular structure of heterocyclic halobismuthanes **1–3**

The Lewis acidity at the bismuth center was essential for generating the activity. Halobismuthanes **1a**, **1b** and **2** showed high antifungal activities, and the activity of monosubstituted **1** decreased as the ClogP value increased, depending on the substituent. Based on this relationship, to achieve higher activity we synthesized **3a** bearing hydrophilic substituents, but its activity was much lower than that of parent **1a**.[15] We attributed this to the considerable decrease in the lipophilicity of **3a**. However, we have not tested this hypothesis experimentally.

We envisaged that replacing one of the benzene rings in **1a** or **2** with a pyridine ring should provide important information about whether the decrease in antifungal activity is related to the hydrophilicity. Pyridine is an isostere of benzene ring and is more hydrophilic than benzene.[17–22] We designed several bismuth heterocycles **4–9** derived from phenyl pyridinyl sulfone (Scheme 2).

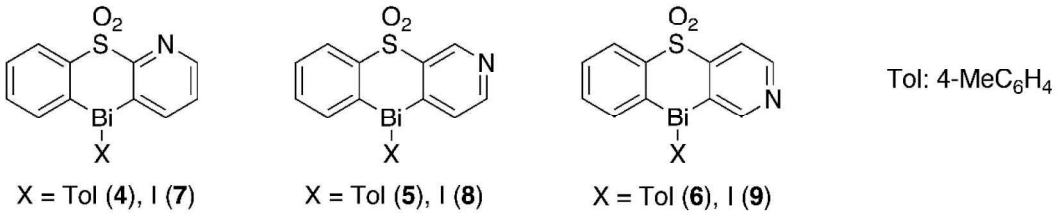

Scheme 2. Molecular structure of bismuth heterocycles **4–9**

This bioisosteric replacement is expected to make **7–9** much more hydrophilic than **2**, although the molecular shape is the same. In this paper, we report the synthesis and antifungal activities of **4–9**. To the best of our knowledge, organobismuth compounds in which the bismuth atom is directly attached to a pyridine skeleton through a bismuth–carbon bond is rare and have been synthesized only recently.[23,24] In contrast, bismuth complexes with pyridine ligands bound through bismuth–nitrogen bonds have been characterized.[25–27]

RESULTS AND DISCUSSION

Synthesis: Phenyl 2-pyridinyl sulfone **10** was prepared by heating 2-bromopyridine and sodium benzenesulfinate in acetic acid.[28] Phenyl 3-pyridinyl sulfone **11**[29] and phenyl 4-pyridinyl sulfone **12**[30] were prepared by heating the corresponding bromopyridine and thiophenol in DMF in the presence of K_2CO_3 followed by the oxidation of the resulting phenyl pyridinyl sulfide.[31]

Our initial efforts were aimed at identifying conditions for the synthesis of **4** (Scheme 3). When **10** (1 mmol) was treated with LTMP (2.2 mmol) in THF at –40 °C for 20 min, an orange suspension was obtained. Addition of $TolBiCl_2$ (1 mmol) to the suspension at –70 °C, followed by workup and subsequent purification of the reaction mixture by chromatography (silica gel) gave **4** (0.68 mmol) in 68% yield along with acyclic **13** (0.048 mmol) in 10% yield as a minor product. The formation of **13** indicates that the pyridine-ring-lithiated intermediate of **10** is stable. Based on this result, we decided to lithiate **11** at a lower temperature because the lithiation of 3-substituted pyridines proceeds at the 4-position owing to the inherent higher acidity of the proton at this position.[32–34] Furthermore, the 4-position of the pyridine ring is susceptible to the unfavorable nucleophilic reaction.[35] When **11** was treated with LTMP at –

55 °C, the solution immediately turned dark red. The reaction with $TolBiCl_2$ gave **5** in 40% yield. In this reaction, the bismuth analog, similar to **13** derived from the monolithiation of **11**, was not detected. Finally, we lithiated **12** under forcing conditions because the synthesis of **4** via the lithiation of **10** at –40 °C gave **13** derived from the monolithiation of **10**. Thus, **12** was lithiated with LTMP at –15 °C, and an orange suspension was obtained that was treated with $TolBiCl_2$ to give **6** in 58% yield without a byproduct, but unreacted **12** was recovered (35%). The recovery of **12** suggests that the pyridine ring proton adjacent to the sulfonyl group of **10** is susceptible to the lithiation compared to that of **12**. Iodination of **4**–**6** afforded the corresponding iodobismuthanes **7**–**9** in high yields together with 4-iodotoluene. This reaction may be rationalized as follows; the oxidative addition of iodine on the bismuth atom gives a pentavalent intermediate, which undergoes the reductive elimination of 4-iodotoluene to form the iodobismuthane. The selective elimination of the tolyl group is understood by the transannular interaction[36,37] between the bismuth and sulfonyl oxygen atoms, which forms the hypervalent O–Bi–I bond.[38] It is known that the transannular interaction promotes the reductive elimination on the pentavalent bismuth atom.[39,40] Furthermore, arsenic halogenation of 9-arsafluorene has shown that the reaction mechanism involves the oxidative addition and reductive elimination on the arsenic atom.[41]

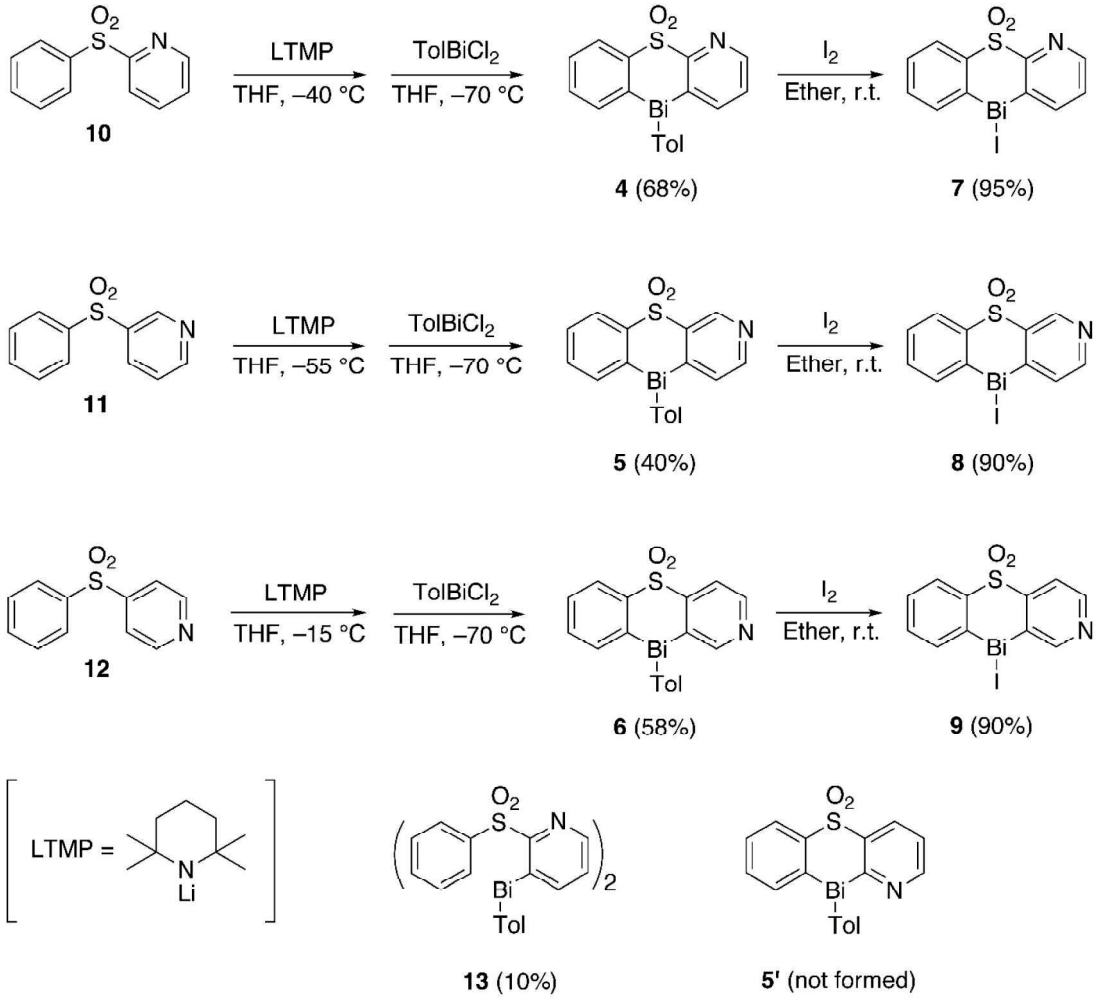

Scheme 3. Synthesis of bismuth heterocycles **4**–**9**

NMR spectroscopic study: The ^{1}H NMR spectrum of compounds **4**–**6** in $CDCl_3$ showed characteristic proton signals due to the pyridine ring, which were used to assign these compounds. Compound **4** possesses only one proton adjacent to the nitrogen of the pyridine ring, whose signal appeared at the highest chemical shift (δ 8.63 ppm) as a double doublet. However, compound **5** showed signals from the two protons adjacent to the nitrogen, excluding the possibility of the formation of isomeric **5′**. In **5**, the signal of the unique pyridine ring proton next to the sulfonyl substituent appeared at a high chemical shift (δ 9.41 ppm) as a singlet owing to the effect of the adjacent nitrogen atom and the sulfonyl group. Compound **6** also

shows the signals due to the two protons adjacent to the nitrogen. The signal for the pyridine ring proton neighboring the bismuth atom was characteristic of this compound and appeared as a singlet at a lower chemical shift (δ 8.84 ppm) than the singlet proton signal (δ 9.41 ppm) for the pyridine ring of **5**. In the ^{1}H NMR spectra of iodobismuthanes **7–9** in $CDCl_3$, the protons adjacent to the bismuth atom in the benzene and pyridine rings underwent anisotropic deshielding because of their close proximity to the iodine atom.[9] Thus, the proton signal of the benzene ring for **7–9** appeared at about δ 9.2 ppm, 1.3 ppm higher than that of parent bismuthanes **4–6**. However, the proton signal of the pyridine ring for **7**, **8** and **9** appeared at higher shifts of δ 9.55, 9.13 and 9.89 ppm, respectively, which are 1.0–1.3 ppm higher than those of parent compounds **4–6**. These observations indicate that the sulfonyl oxygen atom was coordinated to the bismuth atom to form a hypervalent O–Bi–I bond. In the ^{13}C NMR spectra of iodobismuthanes **7**, **8** and **9** in DMSO-d_6, the signal for the ipso carbon attached to the bismuth in the pyridine ring appeared at δ 170.8, 188.4 and 169.7 ppm, respectively, whereas the signal due to the phenyl ipso carbon attached to the bismuth was always observed around δ 180 ppm.

X-Ray structure analysis of 9: We prepared single crystals of **9**. The molecular structure of **9** is shown in Figure 1, and the selected bond lengths, atomic distances and angles are shown in Table 1. This molecule has a chiral bismuth center. Interestingly, we found that only one enantiomer is present in the measured crystal.

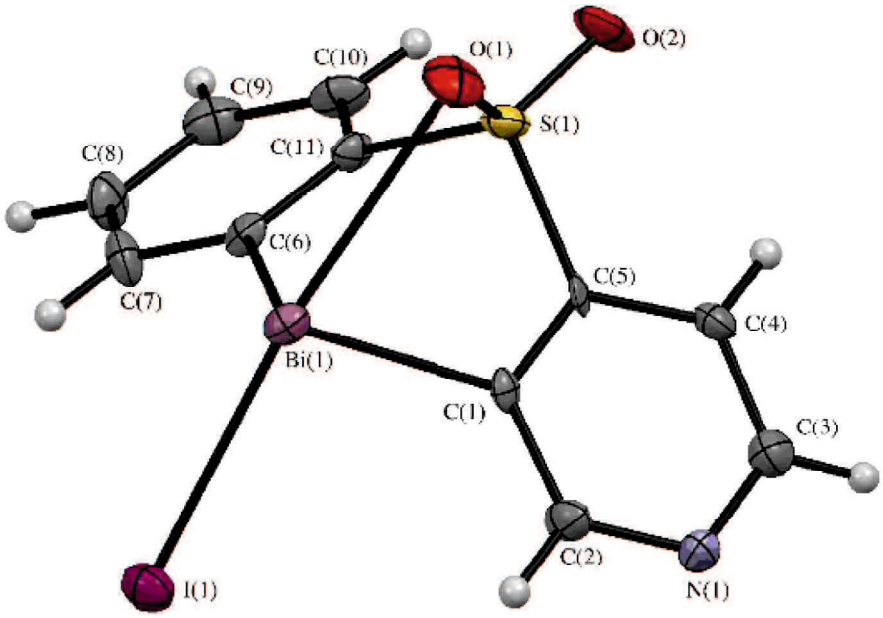

Figure 1. Molecular structure of **9**

The bismuth center adopts a distorted trigonal bipyramidal geometry, where the carbon atoms C(1) and C(6) occupy the equatorial plane with a C(1)–Bi(1)–C(6) angle of 86.1(5)° (Table 1). The apical positions of the distorted trigonal bipyramid are occupied by the sulfonyl oxygen and iodine atoms with an O(1)•••Bi(1)–I(1) angle of 159.0(2)°. The lone pair of electrons is considered to occupy the remaining equatorial position. The intramolecular Bi(1)•••O(1) distance 2.788(9) Å is longer than the sum of the covalent radii (2.10 Å) but much shorter than that of the van der Waals radii (3.72 Å),[42,43] in accord with the formation of a hypervalent bond over the oxygen, bismuth and iodine atoms in **9**. The intermolecular atomic distances between the bismuth and nitrogen atoms and between the bismuth and iodine atoms are both within the sum of the van der Waals radii (3.62 and 4.05Å, respectively),[44] suggesting the existence of a weak interaction.

Table 1. Selected bond lengths (Å), atomic distances (Å) and angles (°) for compound **9**

Bond lengths		Torsion angles	
Bi(1)–I(1)	2.8518(12)	I(1)–Bi(1)–C(1)–C(2)	–43.3(9)
Bi(1)–C(1)	2.293(14)	Bi(1)–C(1)–C(2)–N(1)	–174.4(9)
Bi(1)–C(6)	2.294(14)	Bi(1)–C(1)–C(5)–S(1)	3.7(15)
S(1)–O(1)	1.485(16)	Bi(1)–C(1)–C(5)–C(4)	177.7(8)
S(1)–O(2)	1.435(11)	O(1)–S(1)–C(5)–C(1)	43.9(10)
		O(2)–S(1)–C(5)–C(1)	173.7(8)
		C(1)–Bi(1)–C(6)–C (7)	133.2(10)
Bond angles		**Atomic distances**	
C(1)–Bi(1)–C(6)	86.1(5)	Intramolecular	
I(1)–Bi(1)–C(1)	96.1(3)	Bi(1)•••O(1)	2.788(9)
I(1)–Bi(1)–C(6)	92.8(3)		
O(1)•••Bi(1)–I(1)	159.0(2)	Intermolecular	
Bi(1)–C(1)–C(5)	118.2(10)	Bi(1)•••N(1)	3.252(11)
C(5)–S(1)–C(11)	103.9(7)	Bi(1)•••I(1)	3.877(1)
O(1)–S(1)–O(2)	119.2(6)		

Qualitative antifungal assay: We tested the inhibition activity of iodobismuthanes **7–9** together with triarylbismuthanes **4–6** and **13**. Table 2 summarizes the inhibition activities of these compounds and our previously reported compounds **1–3**. Each compound was dissolved in DMSO at a concentration of 30 mM and 5 μL of each solution was directly spotted on the surface of the agar plate containing the yeast. Iodobismuthanes **7–9** were stable in water and DMSO, indicating that the hypervalent bond formation suppresses the hydrolysis and redistribution reactions of these compounds.

Triarylbismuthanes **4–6** and **13** were inactive, but iodobismuthanes **7–9** showed high antifungal activities. This is consistent with our previous finding that the Lewis acidic bismuth center is the active site.[9,14–16] The activity increased as the nitrogen atom moved further from the sulfonyl group and closer to the bismuth atom. Thus, iodobismuthane **9** showed the highest activity of **7–9** and higher activity than **1a** and **2**. The effect of the position of the nitrogen atom on the activity may imply an efficient secondary interaction of the nitrogen atom with biomolecules that bind to the active bismuth center. It has been reported that replacing the phenyl ring of the core indole with a pyridine ring preserves or substantially reduces the inhibitory activity, depending on the position of the nitrogen atom.[19]

Next, we investigated the effect of concentration of **9** on its antifungal activity. In response to decreasing the concentrations of **9** from 30 to 3.75 mM, the activity decreased (20, 15, 13, and 10 mm for 30, 15, 7.5, and 3.75 mM, respectively). At the lowest concentration (3.75 mM), **9** still showed half of its original activity. Although the activities of **7–9** were not as high as the standard antifungal drug, nystatin, this finding demonstrates the high antifungal activity of organobismuth compounds.

Table 2. Antifungal assay for halobismuthanes and triarylbismuthanes

Compound	Inhibition Zone (mm)	ClogP	Compound	Inhibition Zone (mm)	ClogP
1a	18	1.18	**2**	17	1.18
1b	17	1.45	**3a**	8	0.81
1c	14	1.68	**3b**	0	6.13
1d	13	2.02	**4**	0	3.10
1e	11	1.52	**5**	0	3.10
1f	11	2.28	**6**	0	3.10
1g	7	1.77	**13**	0	6.29
1h	0	3.00	**7**	16	0.29
1i	0	3.06	**8**	19	0.29
1j	8	1.68	**9**	20	0.29
1k	10	2.02	Nystatin	30	–
1l	13	2.02			

We have previously reported the antifungal activity of chlorobismuthanes **1** and related derivatives **3**.[15] A clear structure–activity relationship was observed in **1a–l** ($r = -0.85$, $n = 12$) between the size of the inhibition zone and the value of ClogP, where the antifungal activity increased with decreasing lipophilicity (Table 2). However, **3a** (ClogP = 0.81), which was more hydrophilic, exhibited only low activity compared to **1a**. We attributed this to the considerable

decrease in the lipophilicity of **3a** because the relationship appeared to be applied for the limited range of the ClogP values, depending on the substituent on the benzene ring. In fact, chlorobismuthanes **1h**, **1i** and **3b**, whose value of ClogP was more lipophilic and over 3.00, did not show any antifungal activities despite the presence of the Lewis acidic bismuth center. Hence, taking into account the fact that the activity of **3a** was lower than that of **1a**, it was unexpected that more hydrophilic **7**–**9** (ClogP = 0.29) showed higher activities than **3a**. Furthermore, Figure 2 revealed that application of the data on **2** and **7**–**9** to the plot of **1** improved the linearity of the correlation (r = –0.86, n = 16). Although the reason for the considerable deviation of **3a** from this plot is not clear, it may be attributed to the acidic phenolic hydroxyl substituents which ionize or aggregate through the intermolecular hydrogen bonding, preventing **3a** from passing through the cell membrane of the yeast.

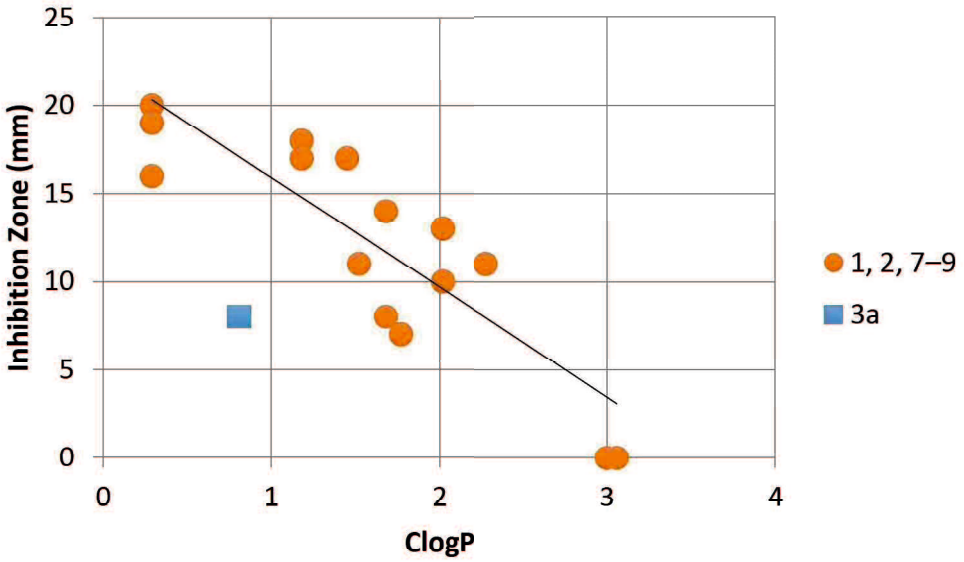

Figure 2. Structure–activity relationship for halobismuthanes **1**, **2**, **3a** and **7**–**9**

DFT study: Recently, we have reported the antifungal activity of hypervalent organobismuth(III) compounds derived from alkyl aryl ketones against *S. cerevisiae*.[9] Bismuthane **14** showed the highest activity comparable to **1a**, but **15** bearing a bulky mesityl

group was inactive (Scheme 4). Furthermore, DFT calculations[45] suggested that the generation of antifungal activity of the bismuthanes was well understood by the nucleophilic addition of a biomolecule at the bismuth atom to give an intermediate ate complex (Table 3).[9] Although we have not identified the biomolecules to which these bismuthanes bind, we expect that the Lewis acidic bismuth atom has a high affinity for thiol groups.[1,46] There was a weak but positive correlation between the antifungal activity and the association energy (enthalpy) in the ate complex formation using methanethiolate anion as a model nucleophile.[9] Thus, the reactions of **1a**, **2** and **14** had high exothermic association energies while no minimum energy path connects the reactants and the product in the reaction of **15** bearing a bulky mesityl group.

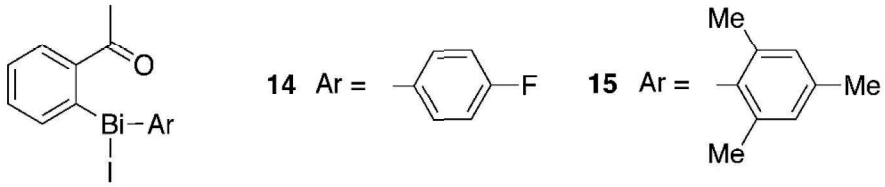

Scheme 4. Structure of iodobismuthanes **14** and **15**

It should be noted that the association energy of **3a** was almost the same as that of **1a**. This indicates that the hydroxyl substituents little affect the ate complex formation of **3a**. Despite this, the loss of the activity in **3a** may be attributed to the behavior of the phenolic hydroxyl substituents mentioned above.

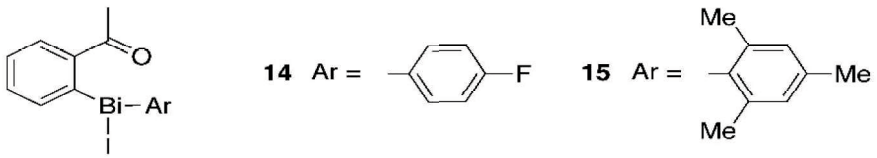

Table 3. Association energy of halobismuthanes

Compound	Inhibition Zone (mm)	Association Energy (kcal/mol)
1a	18	–17.22
2	17	–20.18
3a	8	–17.15
14	19	–16.00
15	0	–
7	16	–20.87
8	19	–21.54
9	20	–21.95

We calculated the association energy of **7–9** by using methanethiolate anion as a model nucleophile (Table 3 and Scheme 5). It is expected that the intramolecular bismuth–oxygen coordination is cleaved by the ate complex formation to form a hypervalent S–Bi–I bond. Iodobismuthanes **7–9** had some of the most exothermic association reactions. Interestingly, the association energy negatively increased in the order **7** < **8** < **9**, which is in good agreement with the order of the antifungal activity. Hence, this association path is preferable to understand the mechanism of action of these iodobismuthanes.

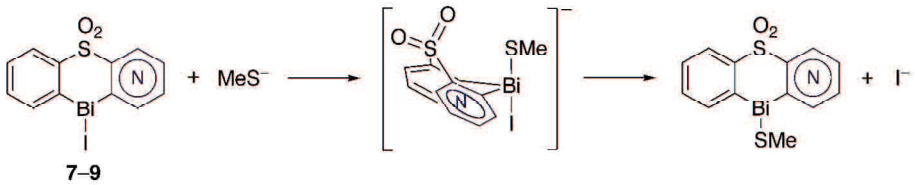

Scheme 5. Plausible association pathway of iodobismuthanes **7–9** using methanethiolate anion

CONCLUSION

The bioisosteric replacement of the phenyl ring of the diphenyl sulfone scaffold by the pyridine ring improved the antifungal activity of the hypervalent halobismuthanes. A clear structure–activity relationship was observed in **1**, **2** and **7**–**9** between the size of the inhibition zone and the value of ClogP. Stabilizing the ate complex appears to be important. The present study provides insights that will aid the design of antifungal hypervalent halobismuthanes by simply estimating the ClogP value and the association energy. Further studies are now underway to find more active halobismuthanes.

EXPERIMENTAL

All reactions were carried out under argon unless otherwise noted. THF and diethyl ether were distilled from benzophenone ketyl before use. Melting points were determined on a YANAGIMOTO melting point apparatus without correction. ^{1}H and ^{13}C NMR spectra were recorded in $CDCl_3$ or DMSO-d_6 on a BRUKER AVANCE 400S spectrometer. Chemical shifts were referenced to residual solvent peak: chloroform (7.26 ppm, 77.0 ppm) and DMSO (2.50 ppm, 40.45 ppm). IR spectra were obtained as KBr pellets on a Nicolet FT-IR Impact 410 spectrophotometer. Elemental analyses were performed on a MICRO CORDER JM10 apparatus (J-SCIENCE LAB. Co.). HRMS were recorded on a Bruker Daltonics micrOTOF II (APCI) instrument. Charts of ^{1}H and ^{13}C NMR spectra of reported compounds are summarized in Supporting Information.

Synthesis of 4 and 13: A mixture of bismuth(III) chloride (211 mg, 0.67 mmol) and tris(4-methylphenyl)bismuthane (162 mg, 0.33 mmol) was stirred in ether (8 mL) at room temperature for 1 h. To a stirred solution of 2,2,6,6-tetramethylpiperidine (0.37 mL, 2.2 mmol) in THF (10 mL) was added dropwise at –78 °C butyllithium (2.2 mmol). After 50 min a solution of **10** (219 mg, 1 mmol) in THF (3 mL) was added at –40 °C and the mixture was stirred for

20 min at this temperature. To this solution was added at –70 °C the suspension of dichloro(4-methylphenyl)bismuthane (ca. 1 mmol) thus formed, and the resulting mixture was stirred for 2 h, during which time the temperature was raised to ambient. The reaction mixture was poured into brine (50 mL) and extracted with ethyl acetate (50 mL × 3). The combined extracts were concentrated to leave an oily residue, which was purified by chromatography (silica gel) using hexane–ethyl acetate (3:1) as the eluent to afford **4** and **13** in 68% yield (352 mg, 0.68 mmol) and 10% yield (35 mg, 0.048 mmol), respectively.

4-Aza-10-(4-methylphenyl)phenothiabismine 5,5-dioxide (4): colorless solid; mp 232–234 °C; ^{1}H NMR (400 MHz, $CDCl_3$): δ 2.35 (3H, s), 7.19 (1H, dd, J = 4.8, 7.4 Hz), 7.26 (2H, d, J = 7.6 Hz), 7.41 (1H, dt, J = 1.2, 7.2 Hz), 7.45 (1H, dt, J = 1.2, 7.2 Hz), 7.63 (2H, d, J = 7.6 Hz), 7.87 (1H, dd, J = 1.2, 7.6 Hz), 8.21 (1H, dd, J = 1.6, 7.2 Hz), 8.43 (1H, dd, J = 1.2, 7.6 Hz), 8.63 (1H, dd, J = 1.6, 4.4 Hz); ^{13}C NMR (100 MHz, $CDCl_3$): δ 21.6, 127.3, 128.3, 129.0, 132.0, 133.8, 137.5, 138.6, 138.9, 141.9, 146.1, 149.0, 151.3 (br), 157.6, 159.2 (br), 163.1 (br). IR (KBr): ν = 1310, 1290, 1160, 1130, 1100, 1080, 1050, 1010, 790, 760, 590 and 570 cm^{-1}. Anal. Calc. for $C_{18}H_{14}BiNO_2S$: C, 41.79; H, 2.73; N, 2.71. Found: C, 41.97; H, 3.03; N, 2.66.

(4-Methylphenyl)bis(2-phenylsulfonylpyridin-3-yl)bismuthane (13): colorless solid; mp 229–231 °C; ^{1}H NMR (400 MHz, $CDCl_3$): δ 2.36 (3H, s), 7.26 (2H, d, J = 7.6 Hz), 7.28 (2H, dd, J − 4.8, 7.4 Hz), 7.43 (4H, t, J − 7.6 Hz), 7.56 (2H, t, J = 7.2 Hz), 7.60 (2H, d, J = 7.6 Hz), 7.86 (4H, d, J = 7.2 Hz), 8.20 (2H, dd, J = 1.6, 7.6 Hz), 8.74 (2H, dd, J = 1.6, 4.4 Hz); ^{13}C NMR (100 MIIz, $CDCl_3$): δ 21.6, 128.9, 129.0 (× 2), 132.3, 133.6, 138.0, 138.1, 139.2, 149.3, 149.7, 157.2 (br), 162.6, 168.5 (br). IR (KBr): ν = 1450, 1300, 1160, 1120, 1080, 770, 750, 740, 710, 690, 590 and 570 cm^{-1}. Anal. Calc. for $C_{29}H_{23}BiN_2O_4S_2$: C, 47.29; H, 3.15; N, 3.80. Found: C, 46.90; H, 3.47; N, 3.79.

3-Aza-10-(4-methylphenyl)phenothiabismine 5,5-dioxide (5): A mixture of bismuth(III) chloride (211 mg, 0.67 mmol) and tris(4-methylphenyl)bismuthane (162 mg, 0.33 mmol) was stirred in ether (8 mL) at room temperature for 1 h. To a stirred solution of 2,2,6,6-tetramethylpiperidine (0.37 mL, 2.2 mmol) in THF (10 mL) was added dropwise at –78 °C butyllithium (2.2 mmol). After 20 min a solution of **11** (219 mg, 1 mmol) in THF (3 mL) was added at –55 °C, and the temperature was lowered to –70 °C immediately. To this solution was added at this temperature the suspension of dichloro(4-methylphenyl)bismuthane (ca. 1 mmol) thus formed, and the resulting mixture was stirred for 2 h, during which time the temperature was raised to ambient. The reaction mixture was poured into brine (50 mL) and extracted with ethyl acetate (50 mL × 3). The combined extracts were concentrated to leave an oily residue, which was purified by chromatography (silica gel) using hexane–ethyl acetate (3:1) as the eluent to afford **5** in 40% yield (207 mg, 0.4 mmol). Colorless solid; mp 224–226 °C; ^{1}H NMR (400 MHz, $CDCl_3$): δ 2.35 (3H, s), 7.27 (2H, d, J = 7.2 Hz), 7.39 (1H, dt, J = 1.2, 7.2 Hz), 7.44 (1H, dt, J = 1.2, 7.2 Hz), 7.63 (2H, d, J = 7.2 Hz), 7.80 (1H, d, J = 4.4 Hz), 7.89 (1H, dd, J = 1.2, 7.2 Hz), 8.42 (1H, dd, J = 1.6, 7.6 Hz), 8.44 (1H, d, J = 4.4 Hz), 9.41 (1H, s); ^{13}C NMR (100 MHz, $CDCl_3$): δ 21.6, 127.4, 128.6, 132.1, 132.3, 133.9, 137.7, 138.6, 138.7, 139.1, 141.2, 146.3, 152.5, 158.9 (br), 162.4 (br), 168.7 (br). IR (KBr): ν = 1550, 1440, 1390, 1300, 1150, 1100, 1080, 1060, 1010, 780, 760, 730, 600, 570, 520 and 460 cm^{-1}. Anal. Calc. for $C_{18}H_{14}BiNO_2S$: C, 41.79; H, 2.73; N, 2.71. Found: C, 41.93; H, 3.09; N, 2.70.

2-Aza-10-(4-methylphenyl)phenothiabismine 5,5-dioxide (6): A mixture of bismuth(III) chloride (211 mg, 0.67 mmol) and tris(4-methylphenyl)bismuthane (162 mg, 0.33 mmol) was stirred in ether (8 mL) at room temperature for 1 h. To a stirred solution of 2,2,6,6-tetramethylpiperidine (0.37 mL, 2.2 mmol) in THF (10 mL) was added dropwise at –78 °C butyllithium (2.2 mmol). After 50 min a solution of **12** (219 mg, 1 mmol) in THF (3 mL) was added at –15 °C, and the mixture was stirred for 10 min at this temperature. To this solution

was added at –70 °C the suspension of dichloro(4-methylphenyl)bismuthane (ca. 1 mmol) thus formed, and the resulting mixture was stirred for 2 h, during which time the temperature was raised to ambient. The reaction mixture was poured into brine (50 mL) and extracted with ethyl acetate (50 mL × 3). The combined extracts were concentrated to leave an oily residue, which was purified by chromatography (silica gel) using hexane–ethyl acetate (3:1) as the eluent to afford **6** in 58% yield (301 mg, 0.58 mmol). Colorless solid; mp 100–102 °C; ^{1}H NMR (400 MHz, $CDCl_3$): δ 2.34 (3H, s), 7.26 (2H, d, J = 7.6 Hz), 7.39 (1H, dt, J = 1.2, 7.2 Hz), 7.44 (1H, dt, J = 1.2, 7.2 Hz), 7.65 (2H, d, J = 7.6 Hz), 7.90 (1H, dd, J = 0.8, 7.6 Hz), 8.17 (1H, d, J = 5.2 Hz), 8.41 (1H, dd, J = 0.8, 7.6 Hz), 8.69 (1H, d, J = 4.4 Hz), 8.84 (1H, s); ^{13}C NMR (100 MHz, $CDCl_3$): δ 21.6, 120.3, 127.8, 128.5, 132.0, 134.0, 137.9, 138.5, 139.0, 140.3, 150.2(× 2) 150.6 (br) 157.4, 158.8 (br), 160.8 (br). IR (KBr): ν – 1540, 1490, 1450, 1390, 1300, 1170, 1150, 1100, 1060, 1010, 790, 750, 730, 690, 590, 570 and 480 cm^{-1}. Anal. Calc. for $C_{18}H_{14}BiNO_2S$: C, 41.79; H, 2.73; N, 2.71. Found: C, 41.81; H, 3.03; N, 2.67.

Synthesis of 7, 8 and 9: A typical example is exemplified by the synthesis of **7**: To a suspension of **4** (104 mg, 0.2 mmol) in diethyl ether (5 mL) was added dropwise a solution of iodine (51 mg, 0.2 mmol) in the same solvent (5 mL) at room temperature until **4** was completely consumed (checked by TLC). The reaction mixture was concentrated to leave solids, which were crystallized from MeOH to give **7**.

4-Aza-10-iodophenothiabismine 5,5-dioxide (7): pale yellow solid; yield 95%; mp > 307 °C; ^{1}H NMR (400 MHz, $CDCl_3$): δ 7.45 (1H, dd, J = 4.8, 7.6 Hz), 7.54 (1H, t, J = 7.6 Hz), 7.69 (1H, t, J = 7.6 Hz), 8.36 (1H, d, J = 7.2 Hz), 8.74 (1H, d, J = 4.8 Hz), 9.21 (1H, d, J = 7.2 Hz), 9.55 (1H, d, J = 7.6 Hz); ^{13}C NMR (100 MHz, DMSO-d_6): δ 128.9, 129.1, 130.3, 136.9, 141.9 (x2), 149.4, 150.3, 158.3, 170.8, 179.6. IR (KBr): ν = 1550, 1300, 1150, 1130, 1100, 1070, 1010, 750, 740, 640, 590, 570, 510 and 460 cm^{-1}. HRMS (APCI): m/z $[M+H]^+$ calcd for $C_{11}H_8BiINO_2S$: 553.9119; found: 553.9110.

3-Aza-10-iodophenothiabismine 5,5-dioxide (8): pale yellow solid; yield 90%; mp 305–307 °C (decomp.); ^{1}H NMR (400 MHz, $CDCl_3$): δ 7.55 (1H, t, J = 7.6 Hz), 7.67 (1H, t, J = 7.2 Hz), 8.38 (1H, d, J = 7.6 Hz), 8.82 (1H, d, J = 4.4 Hz), 9.13 (1H, d, J = 4.8 Hz), 9.22 (1H, d, J = 7.2 Hz), 9.44 (1H, s); ^{13}C NMR (100 MHz, DMSO-d_6): δ 127.6, 129.4, 136.2, 137.0, 139.2, 141.7, 142.1, 145.7, 155.3, 180.2, 188.4. IR (KBr): ν = 1560, 1290, 1150, 1130, 1100, 1080 and 1020 cm^{-1}. HRMS (APCI): *m/z* $[M+H]^+$ calcd for $C_{11}H_8BiINO_2S$: 553.9119; found: 553.9123.

2-Aza-10-iodophenothiabismine 5,5-dioxide (9): pale yellow solid; yield 90%; mp 232–234 °C (decomp.); ^{1}H NMR (400 MHz, $CDCl_3$): δ 7.53 (1H, t, J = 7.2 Hz), 7.67 (1H, t, J = 7.2 Hz), 8.08 (1H, d, J = 4.8 Hz), 8.35 (1H, d, J = 7.6 Hz), 8.84 (1H, d, J = 4.8 Hz), 9.25 (1H, d, J = 7.2 Hz), 9.89 (1H, s); ^{13}C NMR (100 MHz, DMSO-d_6): δ 120.3, 128.0, 129.4, 137.1, 140.8, 142.3, 150.6, 150.7, 161.8, 169.7 (br), 179.6 (br). IR (KBr): ν = 1550, 1390, 1320, 1290, 1270, 1170, 1150, 1120, 1090, 840, 750, 590, 570, 520 and 470 cm^{-1}. Anal. Calc. for $C_{11}H_7BiINO_2S$: C, 23.89; H, 1.28; N, 2.53. Found: C, 23.89; H, 1.50; N, 2.47.

Qualitative antifungal assay: The yeast *S. cerevisiae* W303-1A (*MAT***a** *ade2-1 can1-100 ura3-1 leu2-3,112 trp1-1 his3-11,15*) was used for the qualitative antifungal assay. Yeast extract-peptone-dextrose (YPD) plates contained 1% yeast extract, 2% peptone, 2% glucose and 1.2% agar. The cells were inoculated at a concentration of 1.3×10^4 cells/mL in YPD agar medium at 48 °C and YPD plates were immediately made in Petri dishes. Each compound was dissolved in dimethyl sulfoxide (DMSO) at a concentration of 30 mM and 5 µL of each solution was directly spotted on the surface of the plate. The plates were incubated for 24 h at 30 °C and antifungal activity was indicated by the presence of clear inhibition zones around the spot. The control experiment showed that DMSO does not inhibit fungal growth at all. In order to know the error on the inhibition zone, we carried out the antifungal assay of compounds many times and confirmed that the error was within ±1 mm.

Lipophilicity: The calculated logarithms of water-octanol partition coefficients (ClogP values) were obtained from the ClogP tool in ChemDraw Ultra 11.0 (CambridgeSoft, Cambridge, MA, USA).

DFT calculation of the association energies: The geometries of the bismuth compounds and the corresponding MeS^--adduct anions in Table 3 were fully optimized in water through density functional theory (DFT) calculations within the polarizable continuum model (PCM) using the Gaussian 09 program package.[45] The hybrid B3LYP exchange-correlation functional and 6-31+G*/lanl2dz mixed basis set (lanl2dz effective core potential for bismuth and iodine and 6-31+G* basis set for the remaining atoms) were employed. All d functions in 6-31+G* are pure 5 D basis functions, which is the default form in the Gaussian 09 GenECP calculations. The exothermicity for the nucleophilic addition of MeS^- was calculated from the energies in water of each substrate, in which only the most stable conformer with the lowest energy was considered.

X-Ray crystallographic study: A colorless crystal of **9** was mounted on a glass fiber. All measurements were made with a Rigaku Mercury 70 diffractometer using graphite monochromated Mo-Kα radiation. The data were collected at a temperature of -119 ± 1 °C to a maximum 2θ value of 55.0°. The structure was solved by direct methods[47] and expanded using Fourier techniques. The non-hydrogen atoms were refined anisotropically. All calculations were performed using the CrystalStructure[48] crystallographic software package except for refinement, which was performed using SHELXL Version 2016/6.[49] Crystal data, data collection summary and refinement parameters of **9** are given in Supporting Information. Deposition number CCDC-1836491 for compound **9**. Free copies of the data can be obtained via http://www.ccdc.cam.ac.uk/conts/retrieving.html (or from the Cambridge Crystallographic Data Centre, 12 Union Road, Cambridge, CB2 1EZ, UK; Fax: +44 1223 336033; e-mail: deposit@ccdc.cam.ac.uk).

EXPERIMENTAL DETAILS

A. Crystal Data

Empirical Formula	$C_{11}H_7BiINO_2S$
Formula Weight	553.13
Crystal Color, Habit	colorless, unknown
Crystal Dimensions	0.200 × 0.200 × 0.150 mm
Crystal System	monoclinic
Lattice Type	Primitive
Lattice Parameters	
	a = 8.403(2) Å
	b = 7.854(2) Å
	c = 9.726(2) Å
	ß = 94.689(3)°
	V = 639.8(3) Å^3
Space Group	$P2_1$ (#4)
Z value	2
D_{calc}	2.871 g/cm^3
F_{000}	496.00
λ(Mo-Kα)	163.181 cm^{-1}

B. Intensity Measurements

Diffractometer	Mercury70
Radiation	MoKα (λ = 0.71075 Å)
	Graphite monochromated
Voltage, Current	50kV, 40mA
Temperature	-119.8°C
Detector Aperture	70.0 x 70.0 mm
Data Images	1080 exposures
ω oscillation Range (χ=45.0, ϕ=0.0)	-65.0 115.0°
Exposure Rate	40.0 sec./°
Detector Swing Angle	25.00°
ω oscillation Range (χ=45.0, ϕ=90.0)	-65.0 –115.0°
Exposure Rate	40.0 sec./°
Detector Swing Angle	25.00°
ω oscillation Range (χ=45.0, ϕ=180.0)	-65.0 –115.0°
Exposure Rate	40.0 sec./°
Detector Swing Angle	25.00°
Detector Position	55.01 mm
Pixel Size	0.137 mm
$2\theta_{max}$	55.0°
No. of Reflections Measured Total:	6217
	Unique: 2845 (R_{int} = 0.0527)
	Parsons quotients (Flack × parameter): 809

Corrections	Lorentz-polarization absorption (trans. factors: 0.037–0.086)
C. Structure Solution and Refinement	
Structure Solution	Direct Methods (SIR92)
Refinement	Full-matrix least-squares on F^2
Function Minimized	$\Sigma\, w\,(Fo^2 - Fc^2)^2$
Least Squares Weights	$w = 1/[\,\sigma^2(Fo^2) + (0.0077 \cdot P)^2$ $+ 0.0000 \cdot P\,]$ where $P = (Max(Fo^2,0) + 2Fc^2)/3$
$2\theta_{max}$ cutoff	55.0°
Anomalous Dispersion	All non-hydrogen atoms
No. Observations (All reflections)	2845
No. Variables	154
Reflection/Parameter Ratio	18.47
Residuals: R1 (I>2.00σ(I))	0.0331
Residuals: R (All reflections)	0.0374
Residuals: wR2 (All reflections)	0.0640
Goodness of Fit Indicator	0.799
Flack parameter (Parsons' quotients = 809)	0.039(9)
Max Shift/Error in Final Cycle	0.000
Maximum peak in Final Diff. Map	1.23 e/Å^3
Minimum peak in Final Diff. Map	-2.02 e/Å^3

Table 1. Atomic coordinates and B_{iso}/B_{eq}

atom	x	y	z	B_{eq}
Bi1	0.21706(6)	0.70503(7)	0.10586(5)	1.282(10)
I1	0.04391(13)	0.80381(13)	-0.14590(10)	1.90(2)
S1	0.2727(5)	0.8907(5)	0.4097(4)	1.50(7)
O1	0.3362(10)	0.719(2)	0.3817(10)	2.3(2)
O2	0.3058(13)	0.9643(14)	0.5440(11)	2.3(2)
N1	0.4820(13)	1.205(2)	0.0842(11)	1.9(2)
C1	0.3365(16)	0.9638(17)	0.1505(15)	1.0(2)
C2	0.4028(18)	1.0627(18)	0.0532(16)	1.6(3)
C3	0.4865(17)	1.2634(19)	0.2162(16)	2.0(3)
C4	0.4190(16)	1.1751(18)	0.3201(14)	1.4(3)
C5	0.3446(16)	1.0234(18)	0.2815(15)	1.0(2)
C6	0.0201(16)	0.7994(17)	0.2372(14)	1.2(2)
C7	-0.1387(16)	0.7852(19)	0.1990(16)	1.8(3)
C8	-0.2496(17)	0.846(2)	0.2834(16)	1.9(3)
C9	-0.2051(18)	0.925(2)	0.4069(16)	2.1(3)
C10	-0.0437(18)	0.9441(19)	0.4482(16)	1.8(3)
C11	0.0655(16)	0.8779(19)	0.3633(15)	1.2(3)

$B_{eq} = 8/3\ p^2(U_{11}(aa^*)^2 + U_{22}(bb^*)^2 + U_{33}(cc^*)^2 + 2U_{12}(aa^*bb^*)\cos g + 2U_{13}(aa^*cc^*)\cos b + 2U_{23}(bb^*cc^*)\cos a)$

Table 2. Atomic coordinates and B_{iso} involving hydrogen atoms

atom	x	y	z	B_{iso}
H2	0.39103	1.02727	-0.04048	1.904
H3	0.53782	1.36898	0.23777	2.371
H4	0.42353	1.21614	0.41217	1.654
H7	-0.17322	0.73325	0.11348	2.178
H8	-0.36000	0.83226	0.25579	2.268
H9	-0.28379	0.96622	0.46335	2.486
H10	-0.00957	1.00061	0.53179	2.160

Table 3. Anisotropic displacement parameters

Atom	U_{11}	U_{22}	U_{33}	U_{12}	U_{13}	U_{23}
Bi1	0.0174(3)	0.0141(2)	0.0180(3)	0.0015(3)	0.0056(2)	0.0003(3)
I1	0.0293(6)	0.0239(6)	0.0186(6)	0.0013(5)	-0.0002(5)	-0.0028(5)
S1	0.019(2)	0.027(2)	0.0116(19)	-0.0006(18)	0.0011(16)	0.0057(17)
O1	0.024(6)	0.035(6)	0.029(6)	0.010(8)	-0.006(5)	0.007(7)
O2	0.028(6)	0.050(8)	0.009(6)	0.001(6)	-0.000(5)	0.001(5)
N1	0.027(7)	0.030(6)	0.017(6)	-0.014(9)	0.001(5)	0.002(8)
C1	0.006(7)	0.015(7)	0.015(8)	0.000(6)	0.000(6)	-0.004(6)
C2	0.030(9)	0.018(8)	0.013(8)	-0.004(7)	0.004(7)	-0.003(6)
C3	0.023(9)	0.031(10)	0.021(9)	-0.006(7)	-0.001(7)	0.003(7)
C4	0.019(8)	0.022(10)	0.011(7)	-0.001(7)	-0.002(6)	-0.000(6)
C5	0.006(7)	0.018(8)	0.014(8)	-0.005(6)	-0.003(6)	-0.004(6)

C6	0.021(8)	0.008(7)	0.016(7)	-0.001(7)	0.008(6)	-0.004(6)
C7	0.018(8)	0.024(9)	0.025(9)	-0.003(7)	-0.007(7)	-0.006(7)
C8	0.010(8)	0.032(10)	0.029(10)	-0.002(7)	-0.000(7)	-0.002(7)
C9	0.028(10)	0.026(9)	0.026(10)	0.003(8)	0.007(8)	0.004(8)
C10	0.032(10)	0.022(8)	0.015(8)	0.002(7)	0.012(7)	-0.002(7)
C11	0.010(8)	0.021(8)	0.017(8)	-0.001(6)	0.004(6)	0.004(6)

The general temperature factor expression:

$$\exp(-2p^2(a^{*2}U_{11}h^2 + b^{*2}U_{22}k^2 + c^{*2}U_{33}l^2 + 2a^*b^*U_{12}hk + 2a^*c^*U_{13}hl + 2b^*c^*U_{23}kl))$$

REFERENCES

1. Y. Hong, Y.-T. Lai, G. C.-F. Chan, and H. Sun, *Proc. Natl. Acad. Sci. USA* **2015**, *112*, 3211.
2. T. Hirayama, A. Mukaimine, K. Nishigaki, H. Tsuboi, S. Hirosawa, K. Okuda, M. Ebihara, and H. Nagasawa, *Dalton Trans*. **2017**, *46*, 15991.
3. C. Bonné, A. Pahwa, C. Picard, and M. Visseaux, *Inorg. Chim. Acta*. **2017**, *455*, 521.
4. D. M. Keogan and D. M. Griffith, *Molecules* **2014**, *19*, 15258.
5. H. Li and H. Sun, *Curr. Opin. Chem. Biol.* **2012**, *16*, 74.
6. G. G. Briand and N. Burford, *Chem. Rev.* **1999**, *99*, 2601.
7. Y. C. Ong, V. L. Blair, L. Kedzierski, K. L. Tuck, and P. C. Andrews, *Dalton Trans.* **2015**, *44*, 18215.
8. A. Islam, B. L. Rodrigues, I. M. Marzano, E. C. Perreira-Maia, D. Dittz, M. T. Paz Lopes, M. Ishfaq, F. Frézard, and C. Demicheli, *Eur. J. Med. Chem.* **2016**, *109*, 254.
9. T. Murafuji, M. Tomura, K. Ishiguro, and I. Miyakawa, *Molecules* **2014**, *19*, 11077.
10. K. Onishi, M. Douke, T. Nakamura, Y. Ochiai, N. Kakusawa, S. Yasuike, J. Kurita, C. Yamamoto, M. Kawahata, K. Yamaguchi, and T. Yagura, *J. Inorg. Biochem.* **2012**, *117*, 77.
11. I. P. Ferreira, E. D. L. Piló, A. A. Recio-Despaigne, J. G. Da Silva, J. P. Ramos, L. B. Marques, P. II. D. M. Prazeres, J. A. Takahashi, E. M. Souza-Fagundes, W. Rocha, and H. Beraldo, *Bioorg. Med. Chem.* **2016**, *24*, 2988.
12. D. H. A. Ishak, K. K. Ooi, K.-P. Ang, A. M. Akim, Y.-K. Cheah, N. Nordin, S. N. B. A. Halim, H.-L. Seng, and E. R. T. Tiekink, *J. Inorg. Biochem.* **2014**, *130*, 38.
13. M. Li, Y. Lu, M. Yang, Y. Li, L. Zhang, and S. Xie, *Dalton Trans*. **2012**, *41*, 12882.
14. T. Murafuji, Y. Miyoshi, M. Ishibashi, A. F. M. Mustafizur Rahman, Y. Sugihara, I. Miyakawa, and H. Uno, *J. Inorg. Biochem.* **2004**, *98*, 547.
15. T. Murafuji, Y. Fujiwara, D. Yoshimatsu, I. Miyakawa, K. Migita, and Y. Mikata, *Eur. J. Med. Chem.* **2011**, *46*, 519.

16. T. Murafuji, K. Kitagawa, D. Yoshimatsu, K. Kondo, K. Ishiguro, R. Tsunashima, I. Miyakawa, and Y. Mikata, *Eur. J. Med. Chem.* **2013**, *63*, 531.

17. B. Kelly, M. McMullan, C. Muguruza, J. E. Ortega, J. Javier Meana, L. F. Callado, and I. Rozas, *J. Med. Chem.* **2015**, *58*, 963.

18. K. Miyata, G. Möller, D. Schepmann, and B. Wünsch, *Bioorg. Med. Chem.* **2014**, *22*, 4277.

19. T. Wang, Z. Yin, Z. Zhang, J. A. Bender, Z. Yang, G. Johnson, Z. Yang, L. M. Zadjura, C. J. D'Arienzo, D. DiGiugno Parker, C. Gesenberg, G. A. Yamanaka, Y.-F. Gong, H.-T. Ho, H. Fang, N. Zhou, B. V. McAuliffe, J. Betsy, L. F. Eggers, B. Nowicka-Sans, I. B. Dicker, Q. Gao, R. J. Colonno, P.-F. Lin, N. A. Meanwell, and J. F. Kadow, *J. Med. Chem.* **2009**, *52*, 7778.

20. R. H. Bahekar, M. R. Jain, P. A. Jadav, A. Goel, D. N. Patel, V. M. Prajapati, A. A. Gupta, H. Modi, and P. R. Patel, *Bioorg. Med. Chem.* **2007**, *15*, 5950.

21. D. Laeckmann, F. Rogister, J.-V. Dejardin, C. Prosperi-Meys, J. Géczy, J. Delarge, and B. Masereel, *Bioorg. Med. Chem.* **2002**, *10*, 1793.

22. K. Yoshino, T. Kohno, T. Morita, and G. Tsukamoto, *J. Med. Chem.* **1989**, *32*, 1528.

23. K. Urgin, C. Aubé, C. Pichon, M. Pipelier, V. Blot, C. Thobie-Gautier, E. Léonel, D. Dubreuil, and S. Condon, *Tetrahedron Lett.* **2012**, *53*, 1894.

24. M. Hébert, P. Petiot, E. Benoit, J. Dansereau, T. Ahmad, A. Le Roch, X. Ottenwaelder, and A. Gagnon, *J. Org. Chem.* **2016**, *81*, 5401.

25. S. C. James, N. C. Norman, A. G. Orpen, and J. Starbuck, *Cryst.Eng.Comm.* **2000**, *2*, 67.

26. S. C. James, N. C. Norman, and A. G. Orpen, *J. Chem. Soc., Dalton Trans.* **1999**, 2837.

27. M. Ali, W. R. McWhinnie, A. A. West, and T. A. Hamor, *J. Chem. Soc., Dalton Trans.* **1990**, 899.

28. B. Qu, L. P. Samankumara, J. Savoie, D. R. Fandrick, N. Haddad, X. Wei, S. Ma, H. Lee, S. Rodriguez, C. A. Busacca, N. K. Yee, J. J. Song, and C. H. Senanayake, *J. Org. Chem.* **2014**, *79*, 993.

29. N. Margraf and G. Manolikakes, *J. Org. Chem.* **2015**, *80*, 2582.

30. J. Zou, F. Li, F. G. Tao, *Chin. Chem. Lett.* **2009**, *20*, 17.

31. W. G. Trankle and M. E. Kopach, *Org. Process Res. Dev.* **2007**, *11*, 913.

32. G. Rouquet, D. C. Blakemore, and S. V. Ley, *Chem. Commun.* **2014**, *50*, 8908.

33. G. Deguest, A. Devineau, L. Bischoff, C. Fruit, and F. Marsais, *Org. Lett.* **2006**, *8*, 5889.

34. N. Furukawa, T. Shibutani, and H. Fujihara, *Tetrahedron Lett.* **1989**, *30*, 7091.

35. A. I. Meyers and R. A. Gabel, *Heterocycles* **1978**, *11*, 133.

36. K. Ohkata, M. Ohnishi, and K.-y. Akiba, *Tetrahedron Lett.* **1988**, *29*, 5401.

37. K. Ohkata, S. Takemoto, M. Ohnishi, and K.-y. Akiba, *Tetrahedron Lett.* **1989**, *30*, 4841.

38. H. Suzuki, T. Murafuji, and N. Azuma, *J. Chem. Soc., Perkin Trans 1* **1992**, 1593.

39. M. Minoura, Y. Kanamori, A. Miyake, and K.-y. Akiba, *Chem. Lett.* **1999**, *28*, 861.

40. N. Sakurai, and T. Mukaiyama, *Chem. Lett.* **2007**, *36*, 928.

41. S. Tanaka, H. Imoto, T. Yumura, and K. Naka, *Organometallics* **2017**, *36*, 1684.

42. T. Murafuji, T. Mutoh, K. Satoh, K. Tsunenari, N. Azuma, and H. Suzuki, *Organometallics* **1995**, *14*, 3848.

43. A. Bondi, *J. Phys. Chem.* **1964**, *68*, 441.

44. M. Mantina, A. C. Chamberlin, R. Valero, C. J. Cramer, and D. G. Truhlar, *J. Phys. Chem. A* **2009**, *113*, 5806.

45. M. J. Frisch, G. W. Trucks, H. B. Schlegel, G. E. Scuseria, M. A. Robb, J. R. Cheeseman, G. Scalmani, V. Barone, B. Mennucci, and G. A. Petersson, *et al.* Gaussian 09, Revision C.01; Gaussian, Inc.: Wallingford, CT, USA, **2010**.

46. N. Burford, M. D. Eelman, D. E. Mahony, and M. Morash, *Chem. Commun.* **2003**, 146.

47. SIR92: A. Altomare, G. Cascarano, C. Giacovazzo, and A. Guagliardi, *J. Appl. Cryst.* **1993**, *26*, 343.

48. CrystalStructure 4.1: Crystal Structure Analysis Package; Rigaku Corporation (**2000-2014**). Tokyo 196-8666, Japan.

49. SHELXL Version 2016/6: G. M. Sheldrick, *Acta Cryst.* **2008**, *A64*, 112.

Chapter 3

ONE-POT SYNTHESIS OF HYPERVALENT DIARYL(IODO)BISMUTHANES FROM *O*-CARBONYL IODOARENES BY ZINCATION AND THEIR ANTIFUNGAL ACTIVITIES

Abstract

A convenient one-pot synthetic method for diaryl(iodo)bismuthanes possessing a hypervalent C=O•••Bi–I bond was developed by using arylzinc reagents generated from *o*-carbonyl iodobenzenes and zinc powder under ultrasound sonication. This method was quite superior to the conventional synthetic methods using organolithium and Grignard reagents because the reaction conditions were very mild and did not need low temperature in generating the zinc reagents and formyl and acetyl substituents were not required for their protection. Furthermore, the intermediacy of triarylbismuthane as a precursor for the carbonyl-functionalized hypervalent iodobismuthanes was unnecessary. The antifungal study on these iodobismuthanes against the yeast *Saccharomyces cerevisiae* revealed that the iodobismuthanes bearing an acetyl substituent were the most active and that the introduction of a fluoro substituent into the aromatic ring enhanced the activity.

1. INTRODUCTION

Hypervalent bismuth(III) compounds represent an important class of fundamental organometallics in main group chemistry.[1,2] Intramolecular coordination of a neutral donor to a bismuth(III) center is one of a common methods used for the hypervalent bond formation.[3] Formyl, acetyl and ester groups can play this role by the coordination of the carbonyl oxygen atom. We have previously reported the synthesis of triarylbismuthanes **1** and **2** *ortho*-functionalized with an acetyl and a formyl substituent, respectively, and their transformation

to hypervalent halobismuthanes **3**–**6** (Scheme 1).[4] An X-ray structure analysis of **3** (Ar = Tol, X = Br) revealed the formation of a hypervalent O–Bi–Br bond by the intramolecular coordination of the carbonyl group with the bismuth atom. The hypervalent bond formation was clearly reflected on the change in the spectroscopic characteristics of the carbonyl group in the ^{13}C NMR and IR spectra.

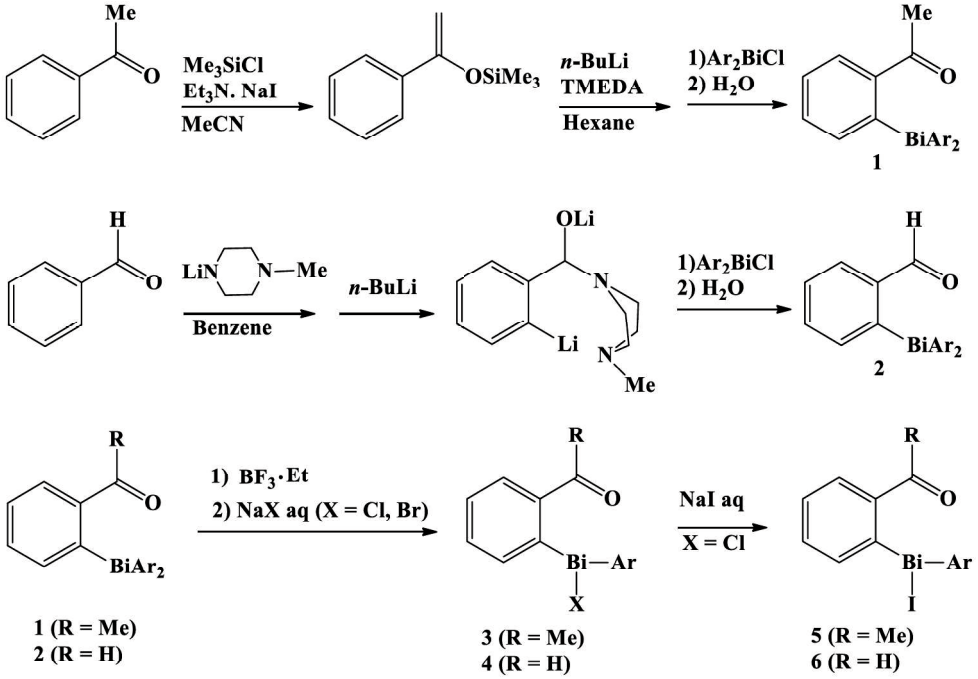

Scheme 1. Synthetic routes to **1**–**6**

Biologically active bismuth compounds have been the subject in medicinal chemistry owing to its minimally low toxic heavy element.[5,6] In this regard, inorganic bismuth complexes have been extensively investigated and their history of medicinal application is very long, whereas there have been limited studies of organobismuth compounds.[7–10] Recently, we have reported that **3** and **5** bearing an acetyl substituent showed moderate to high antifungal activities against the yeast *Saccharomyces cerevisiae*.[11] The activity was sensitive to the nature of the aryl (Ar)

and halo (X) groups. Through this study, we were interested in this result and aimed to find more active derivatives of carbonyl-functionalized halobismuthanes.

Unfortunately, the synthetic methods for **3**–**6** have many drawbacks (Scheme 1).[4,11] Firstly, the synthesis of **3**–**6** needs the route via **1** and **2** because the *ortho*-functionalized aryllithiums are too reactive to react with $ArBiX_2$ to give **3**–**6** directly. Secondly, the carbonyl functionalities of **1** and **2** are incompatible with aryllithiums and have to be protected in the form of silyl enol ether and lithium α-amino alkoxide, respectively. Thirdly, the directed *ortho*-lithiation of these protected intermediates requires an excess amount of *n*-BuLi, which sometimes causes the loss of Ar_2BiCl or decomposition of the intermediate precursors of **1** and **2** by the overreaction with unreacted n-BuLi. In this regard, the lithium α-amino alkoxide has a possibility to react with Ar_2BiCl, giving an undesired bismuth alkoxide. These drawbacks not only make the yields of **1** and **2** low and the synthesis of **3**–**6** unreliable and tedious, but also hamper the design and synthesis of new antifungal halobismuthanes possessing carbonyl functionality. Therefore, an alternative easy and simple synthetic method with high carbonyl group tolerance is highly desired.

We have reported the synthesis of triarylbismuthanes **7** and **8**, each arene being substituted with a formyl or an ester substituent at the *p*-position, by using iodine–magnesium exchange reaction (Scheme 2).[12] The imino and ester substituents were compatible with the respective Grignard reagents despite their polarized double bonds, and the reaction conditions were very mild compared to those in the synthesis of **1** and **2** using the directed lithiation. This led us to use milder organometallic reagent than lithium and magnesium reagents.

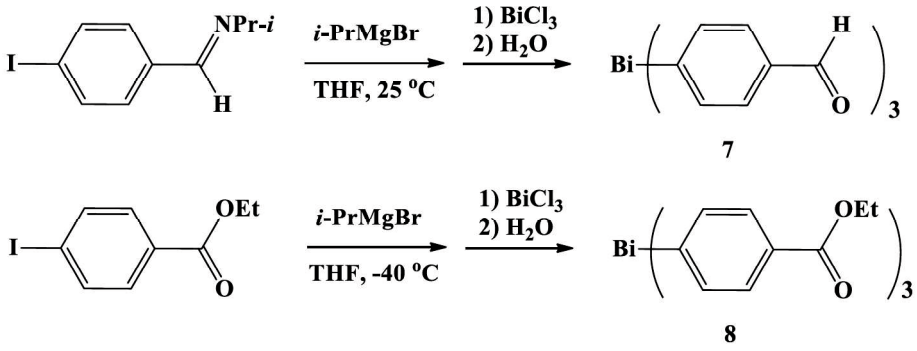

Scheme 2. Synthesis of **7** and **8**

Several alternative methods have been reported for bismuth–carbon bond formation reaction, which include the treatment of aryl iodide with bismuth shots in the presence of Cu and CuI by ball mill technique,[13] the arylation of bismuth(III) carboxylates by sodium tetraarylborate,[14] and the reaction of $BiCl_3$ and organozinc reagents.[15] We focused on the organozinc reagents since they have high functional group tolerance compared to organolithium and Grignard reagents. It has been reported that carbonyl functionality is compatible with organozinc reagents.[16–18] Hence, if one-pot synthesis of the hypervalent halobismuthanes bearing a carbonyl group is established, such method should be highly useful. Herein, we report the synthesis of hypervalent iodobismuthanes **5a**, **6a** and **9–13** functionalized with a carbonyl group by using the zincation of the corresponding iodoarene (Scheme 3). We found that the organozinc method was superior to the previously reported organolithium and Grignard methods for the synthesis of these bismuthanes in the high functional group tolerance, short synthetic step, mild reaction conditions and acceptable yields of the products.

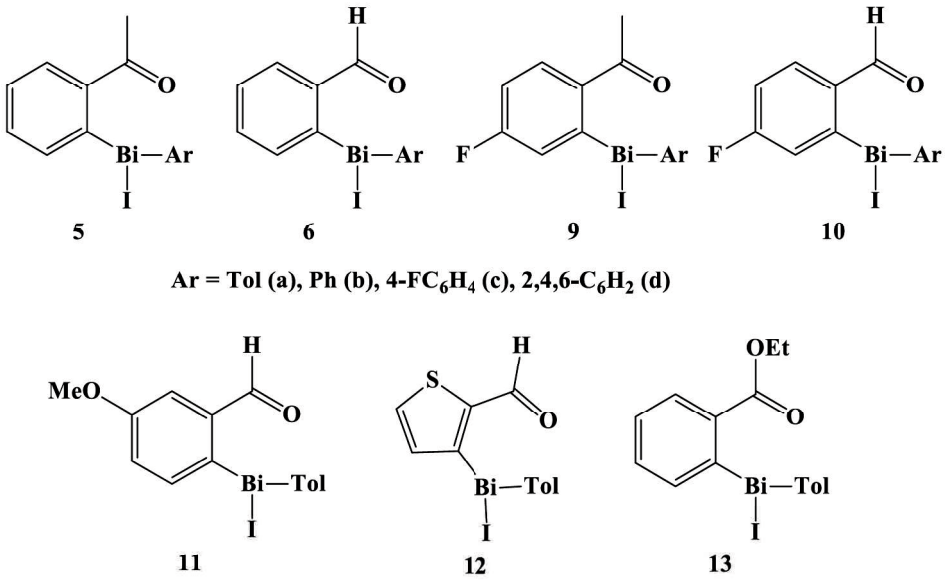

Scheme 3. Hypervalent iodobismuthanes functionalized with a carbonyl group

2. RESULTS AND DISCUSSION

2.1 One-pot synthesis of hypervalent iodobismuthanes

Initially, we tried the one-pot synthesis of **13** by the zincation of ethyl 2-iodobenzoate. The arylzinc was prepared by reference to the method reported by Takagi and co-workers,[16] who treated iodoarenes containing an electron-withdrawing substituent such as a methoxycarbonyl or an acetyl substituent at the ortho position in the presence of zinc powder under ultrasound at 30 °C. When a mixture obtained by the sonication of ethyl 2-iodobenzoate with zinc powder (1 equiv) at 25 °C in DMF was allowed to react with $TolBiCl_2$ (1 equiv), **13** was obtained in only 4% yield (Table 1, Entry 1). The poor yield was attributed to the incomplete conversion of the starting iodoarene to the arylzinc. The yield of **13** increased with increasing the equivalents of both zinc powder and $TolBiCl_2$ (Entries 2 and 3). Furthermore, an increase in the temperature by itself from 25 °C to 48 °C by the sonication accelerated the zincation reaction (Entries 4–9). In this context, we observed that the color of the reaction mixture changed to dark yellow with progress of the zincation, which was a good indication for its

completion. The loading amount of zinc powder was sensitive to the yield of **13** and the best result was obtained when 4 equivalents of zinc powder and 2 equivalents of $TolBiCl_2$ were used (Entry 7). Further loading of zinc powder or $TolBiCl_2$ decreased the yield of **13** (Entries 8 and 9).

Table 1. Optimization of the reaction conditions for the synthesis of **13**

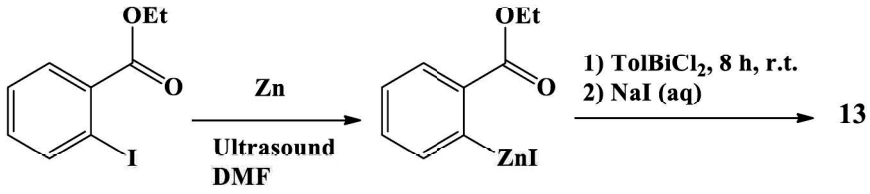

Entry	Zn (equiv)	$TolBiCl_2$ (equiv)	Ultrasound Temp (°C)	Ultrasound Time (h)	Yield (%) **13**
1	1.0	1.0	25	6	4
2	1.5	1.0	25	6	9
3	2.0	1.5	25	5	14
4	2.5	1.5	25–48	3	18
5	3.0	2.0	25–48	4	28
6	3.5	2.0	25–48	4	41
7	4.0	2.0	25–48	4	61
8	4.5	2.0	25–48	5	60
9	4.0	3.0	25–48	5	55

Encouraged by the success in the synthesis of **13**, we next challenged the one-pot synthesis of **5a** and **6a** by application of the reaction conditions used in the synthesis of **13** (Entry 7 in Table 1). Thus, after each mixture of the zincation was colored in dark yellow, the reaction of the

resulting mixture with $TolBiCl_2$ followed by quenching with a saturated aqueous solution of NaI gave **5a** and **6a** in 35% and 56% yields, respectively (Table 2).

Finally, we tried the one-pot synthesis of **9a**, **10a, 11** and **12**. All the synthetic reactions proceeded smoothly to give the corresponding iodobismuthanes in acceptable yields. It should be emphasized that the synthesis of these iodobismuthanes is difficult by the conventional lithiation method shown in Scheme 1 because the fluoro and methoxy substituents act as directed lithiation groups and the thienyl ring proton α to the sulfur atom undergoes undesired lithiation.

Table 2. Synthesis of iodobismuthanes

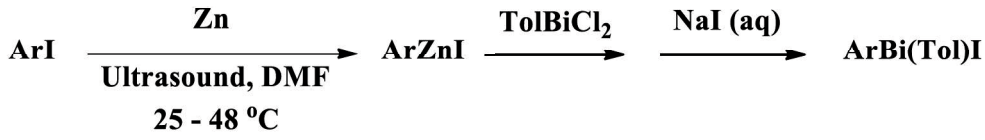

Entry	ArI	Ultrasound Time (h)	$TolBiCl_2$ Time (h)	ArBi(Tol)I	Yield (%)
1	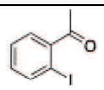	2.0	3.5	**5a**	35
2		3.5	8	**6a**	56
3	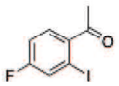	1.5	5	**9a**	28
4	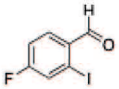	3.0	8	**10a**	29
5	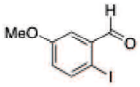	3.5	8	**11**	31
6		4.0	8	**12**	53

The ^{1}H-NMR spectrum of **5a** in $CDCl_3$ showed the anisotropic deshielding of the *ortho* proton adjacent to the bismuth atom in the arylcarbonyl scaffold because of its close proximity to the electronegative iodine atom by the hypervalent O–Bi–I bond formation.[11] Thus, the *ortho* proton signal appeared at δ 9.42 ppm in $CDCl_3$. This was also in the case of **13**, which showed the *ortho* proton signal at δ 9.43 ppm in $CDCl_3$, indicating the formation of the hypervalent bond. In DMSO-d_6, the *ortho* proton signal of **5a** appeared upfield at δ 9.10 ppm, suggesting that the intramolecular Bi–O coordination is weakened by the coordination of the solvent molecule to the bismuth center.

2.2 Growth inhibition tests against *S. cerevisiae*

We have reported that **3** and **5** bearing an acetyl substituent showed moderate to high antifungal activities against the yeast *Saccharomysces cerevisiae*. In this study our interest was focused on the effect of the formyl, ester and fluoro substituent on the antifungal activities. For this purpose, we tested the inhibition activity of iodobismuthanes **6a**, **9a, 10a** and **11–13**. Table 3 summarizes the inhibition activities of these compounds and our previously reported compounds **5**, **14** and **15**. Each compound was dissolved in DMSO at a concentration of 30 mM and 5 μL of each solution was directly spotted on the surface of the agar plate containing the yeast. They showed moderate to high activities. This is consistent with our previous finding that the Lewis acidic bismuth center is the active site.[11,19-21] Although the activities of these iodobismuthanes were not as high as the standard antifungal drug, nystatin, this finding demonstrates the high antifungal activity of organobismuth compounds. Formyl-substituted iodobismuthanes **6a, 10a, 11** and **12** showed lower ClogP values than acetyl-substituted iodobismuthanes **5** and **9a** and ester-substituted iodobismuthane **13**.

Table 3. Antifungal assay for iodobismuthanes

Compound	Inhibition Zone (mm)	ClogP
6a	12	2.11
9a	16	3.34
10a	12	2.25
11	11	2.02
12	11	1.76
13	11	4.18
5a	15	3.12
5b	17	2.63
5c	19	2.77
5d	0	4.12
14	10	3.34
15	13	3.12
Nystatin	30	

Based on this study, the structure–activity relationship of the hypervalent iodobismuthanes may be summarized as follows. Firstly, the comparison of the activities between **5a**, **6a** and **13** indicates that the acyl group attached to the benzene ring is a key functionality that governs the activity. This finding is consistent with our previous result that the long chain (*n*-PrCO, *n*-BuCO) or branched (*i*-PrCO) acyl group much lowers the activity compared to **5a**.[11] Secondly, the activities of formyl-substituted iodobismuthanes **6a**, **10a, 11** and **12** were insensitive to the substituent effect on the benzene ring and to the aromatic ring scaffold because their activities are almost equivalent. This is in contrast to the acetyl-substituted chlorobismuthane **14**, which showed a decreased activity compared to **15** by replacement of the *para* position by the

methoxy substituent (Scheme 4).[11] Thirdly, **9a** bearing an acetyl substituent showed a high activity, which was a little higher than that of **5a**. The design of **9a** was based on the fact that iodobismuthane **5c** showed a higher activity than **5b**. Such an enhancement of the activity by fluoro substituent may be understood by the bioisosteric relationship of fluorine atom with hydrogen atom.[22,23] Hence, we were interested in how the replacement of the Tol group in **9a** by a *p*-FC_6H_4 group affects the antifungal activity of **9c**. We are now trying to synthesize **9c** along with **9b** for comparison.

Formyl-substituted iodobismuthanes **6a, 10a, 11** and **12** showed lower ClogP values than acetyle-substituted iodobismuthanes **5** and **9** and ester-substituted iodobismuthane **13**. Taking into account the good structure-activity relationship between the antifungal activity and the ClogP in the diaryl sulfone system,[24] it is expected that the formyl derivatives show higher activities than the other derivatives.

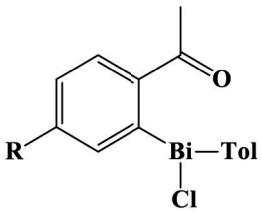

14 (R = MeO)
15 (R = H)

Scheme 4. Structure of **14** and **15**

2.3 DFT study

2.3.1 Ate complex formation of 6 and 9–13

Recently, we have revealed by DFT calculations[25] that the generation of antifungal activity of the hypervalent bismuthanes was well understood by the nucleophilic addition of a biomolecule at the bismuth atom to give an intermediate ate complex.[11,24] Although we have not identified

the biomolecules to which these bismuthanes bind, we expect that the Lewis acidic bismuth atom has a high affinity for thiol groups.[5,26] There was a positive correlation between the antifungal activity and the association energy (enthalpy) in the ate complex formation using methanethiolate anion as a model nucleophile. Thus, the reactions of **5a–c** had high exothermic association energies while no minimum energy path connects the reactants and the product in the reaction of **5d** bearing a bulky mesityl group (Table 4). It is expected that the intramolecular bismuth–oxygen coordination is cleaved by the ate complex formation to form a hypervalent S–Bi–I bond. From these results, it seems that an electron-withdrawing fluoro substituent stabilizes the ate complex whereas the bulky aryl group blocks its formation. We calculated the association energy of **6** and **9–13** by using methanethiolate anion as a model nucleophile (Table 4). Iodobismuthanes **6** and **10–12** bearing a formyl substituent had some of the most exothermic association reactions. This suggests that a weak intramolecular coordination of the formyl substituent compared to the acetyl substituent makes the formation of the ate complex with methanethiolate anion easy to take place. In particular, the highest value of thienyl-ring substituted bismuthane **12** may be understood if we consider that the Bi–O intramolecular distance in the five-membered thienyl ring of **12** is longer than that in the six-membered benzene ring of **6a**, **10a** and **11**. On the contrary to our expectation, however, all the formyl-functionalized iodobismuthanes showed only moderate activities that were almost equivalent. This may be attributed to the deactivation of these bismuthanes induced by the dissociation of the intramolecular Bi–O coordination, i.e., the hydrolysis at the bismuth center to form insoluble polymeric substances containing Bi–O bonds or the disproportionation reaction. In fact, **6a** is expected to be susceptible to hydrolysis compared to **5a** since the coordination ability of a formyl oxygen atom is weaker than that of an acetyl oxygen atom. Another probable route for the deactivation is through the hydration of the formyl substituent followed by the cyclization of the resulting hydroxyl substituent with the bismuth center, leading to a cyclic ate

complex of bismuth alkoxide after deprotonation. These deactivation reactions hinder the ate complex formation of the original iodobismuthanes with methanethiolate because bismuth alkoxides form a rigid dimer or more complex three-dimensional organometallics by the intermolecular Bi–O coordination.[27] To get information about the deactivation, we measured the ^{1}H-NMR spectrum of **6a** in DMSO-d_6–D_2O. Decomposition of **6a** took place to give insoluble substances and the proton signals due to the corresponding hydrate could not be observed. In contrast, no decomposition was observed in the ^{1}H-NMR spectrum of **5a** in DMSO-d_6-D_2O. Taking into account the coordination ability of DMSO-d_6, the coordination of a DMSO-d_6 molecule to the bismuth atom assists the dissociation of the intramolecular Bi–O coordination bond, making the antifungal activities of iodobismuthanes **6a**, **10a**, **11** and **12** moderate and less sensitive to their structure by their hydrolysis or disproportionation. Furthermore, the antifungal activity of **13** was also low despite its association energy that is comparable to that of **5c**. Although the reason is not clear, this may be also attributed to its decomposition because **13** gradually decomposed.

Table 4. Association energy of halobismuthanes

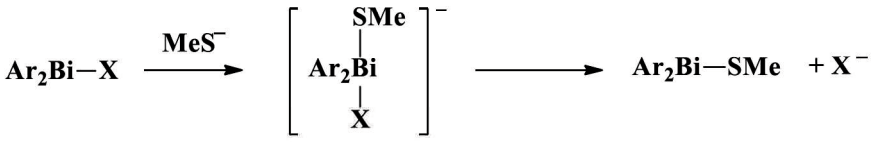

Compound	Inhibition Zone (mm)	ClogP	Association Energy (kcal/mol)
6a	12	2.11	-17.40
9a	16	3.34	-15.57
10a	12	2.25	-17.86
11	11	2.02	-17.29
12	11	1.76	-19.16
13	11	4.18	-16.43
5a	15	3.12	-15.13
5b	17	2.63	-15.43
5c	19	2.77	-16.00
5d	0	4.12	-
14	10	3.34	-11.32
15	13	3.12	-12.00
Nystatin	30		

2.3.2 Estimation of association energy of various acetyl-functionalized iodobismuthanes bearing a heteroaromatic ring scaffold

We found that acetyl-functionalized iodobismuthanes such as **5** and **9** showed the high antifungal activities. In order to search more active compounds, we designed the various acetyl-functionalized heteroaromatic iodobismuthanes and estimated their association energies by using DFT calculation. The relative energy and the intramolecular Bi–O distance were also estimated. The results are shown in Schemes 5–7.

Benzene

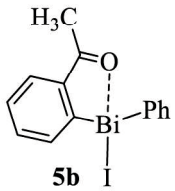

5b

R(Bi-O)	2.422
association energy	-15.43 kcal/mol
	ClogP 2.63 and IZ 17mm

B3LYP/LanL2DZ,6-31+G(d) 5D SCRF(solvent=watcr)

Furans

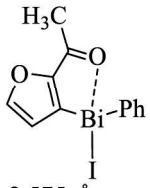

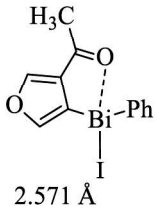

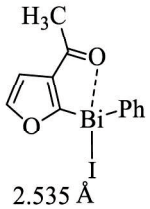

R(Bi-O)	2.575 Å	2.571 Å	2.535 Å
relative energy	(0)	0.86 kcal/mol	2.59 kcal/mol
association energy	-20.13 kcal/mol	-19.51 kcal/mol	-20.63 kcal/mol
	ClogP 1.80	ClogP 1.80	ClogP 1.80

Thiophenes

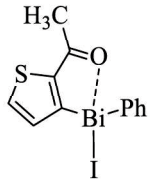

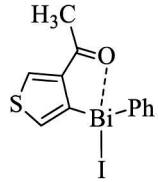

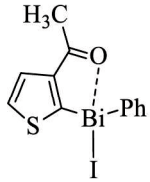

R(Bi-O)	2.480Å	2.509Å	2.470Å
relative energy	1.37 kcal/mol	1.17 kcal/mol	(0)
association energy	-17.70 kcal/mol	-19.11 kcal/mol	-16.65 kcal/mol
	ClogP 2.40	ClogP 2.40	ClogP 2.40

Pyrroles

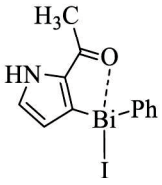

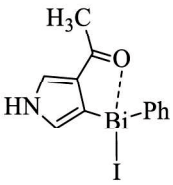

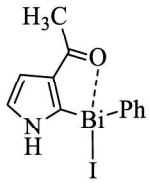

R(Bi-O)	2.498 Å	2.494 Å	2.465 Å
relative energy	1.34 kcal/mol	0.32 kcal/mol	(0)
association energy	-17.56 kcal/mol	-17.06 kcal/mol	-17.76 kcal/mol
	ClogP 1.64	ClogP 1.64	ClogP 1.64

Scheme 5. Association energy of iodobismuthanes derived from acetylheteroles

It should be noted that all the heteroaromatic iodobismuthanes showed negatively higher association energies than acetophenone-based iodobismuthane **5b** (–15.43 kcal/mol). There

seems to be a tendency that the association energy negatively increases with increasing the intramolecular Bi–O distance. This suggests that the ate complex formation is favored in the iodobismuthanes whose carbonyl oxygen atom loosely coordinates to the bismuth center. Thiophene-based iodobismuthanes showed energies different from each other, and the bismuthane whose bismuth atom is attached to the α-position toward the sulfur atom showed the lowest value (–16.65 kcal/mol) not only in the thiophene system but also in all the heteroaromatic iodobismuthanes. The reason may be attributed to the stabilizing effect by the sulfur atom[28,29] since such a tendency of lowering the energy was not seen in the other homologues of the heteroaromatic iodobismuthanes. The association energies of azole-based iodobismuthanes were the highest (–22.90 and –22.57 kcal/mol) in all the heteroaromatic iodobismuthanes. Furthermore, their ClogP values were very hydrophilic. From these findings, it is expected that these azole-homologues have a possibility to show higher activities than **5b**. Hence, it is essential to test the antifungal activity of these azole- and thiophene-based homologues in future. These compounds are possible to synthesize if the zincation is applied.

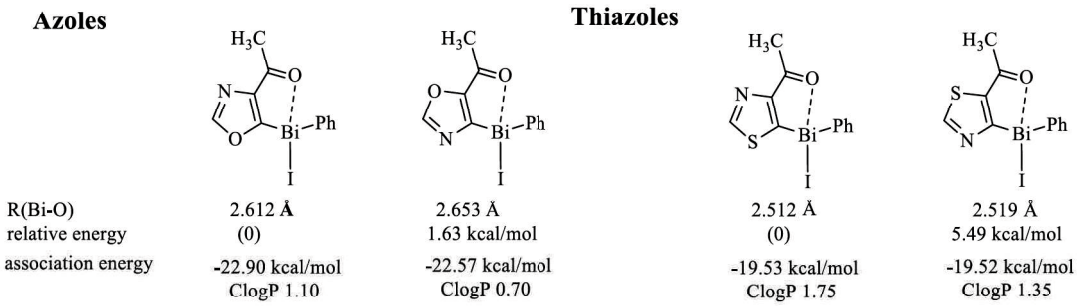

Scheme 6. Association energy of iodobismuthanes derived from acetylazoles and acetylthiazoles

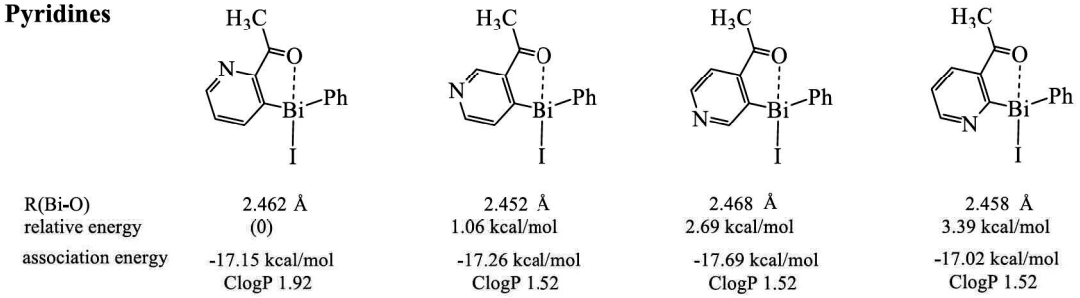

Scheme 7. Association energy of iodobismuthanes derived from acetylpyridines

3 CONCLUSION

Hypervalent iodobismuthanes functionalized with a carbonyl group could be synthesized quite easily by one-pot reaction using arylzinc reagents. Acetyl-functionalized iodobismuthanes showed high activities, which increased by introducing a fluoro substituent into the benzene ring. The DFT calculation suggested that the azole scaffold could be a candidate for more active iodobismuthanes.

4 EXPERIMENTAL

General methods

All of the reactions were carried out under argon unless otherwise noted. *N*,*N*-Dimethylformamide (DMF) and 1,4-dioxane were distilled from calcium hydride. Diethyl ether was distilled from benzophenone ketyl before use. ^{1}H and ^{13}C NMR spectra were recorded in $CDCl_3$ or DMSO-d_6 on a BRUKER AVANCE 400S spectrometer. Chemical shifts were referenced to residual solvent peak: chloroform (7.26 ppm, 77.0 ppm) and DMSO (2.50 ppm, 40.45 ppm). IR spectra were obtained as KBr pellets on a Nicolet FT-IR Impact 410 spectrophotometer. Melting points were determined on a YANAGIMOTO melting point apparatus without correction. Elemental analysis was performed on a MICRO CORDER JM10 apparatus (J-SCIENCE LAB. Co.). HRMS were recorded on a Bruker Daltonics micrOTOF II

(APCI) instrument. 2′-Iodoacetophenone and ethyl 2-iodobenzoate were commercially available. 2-Iodobenzaldehyde, 4-fluoro-2-iodobenzaldehyde, 2-iodo-5-methoxybenzaldehyde, 4-fluoro-2-iodoacetophenone and 3-iodothiophene-2-carboxaldehyde were prepared in high yields by Finkelstein reaction of the corresponding bromoarenes in accordance with the literature.[30]

Typical procedure for the Finkelstein reaction of bromoarenes

To a round-bottomed flask (50 mL) equipped with a magnetic stir bar were added bromoarene (2.5 mmol), CuI (5 mol%), NaI (5 mmol) and 1,3-diaminopropane (10 mol%). After dry 1,4-dioxane (2.5 mL) was added to the flask, the mixture was refluxed for 24 h. The reaction was quenched with water (30 mL) at room temperature and the resulting mixture was extracted with ethyl acetate (3 × 30 mL). The organic layer was dried (Na_2SO_4) and concentrated to leave a residue, which was chromatographed on silica gel with hexane–ethyl acetate (5:1) to give the corresponding iodoarene, which was used in the next step without further purification.

2-Iodobenzaldehyde

Yield 99% (574 mg, 2.48 mmol), Colorless solid, mp 39–41 °C. ^{1}H NMR (400 MHz, $CDCl_3$): δ 7.29 (1H, dt, J = 7.6 Hz, 3.2 Hz), 7.47 (1H, t, J = 7.6 Hz), 7.89 (1H, dd, J = 7.6 Hz, 1.6 Hz), 7.96 (1H, d, J = 8.0 Hz), 10.01 (1H, s).

4-Fluoro-2-iodobenzaldehyde

Yield 97% (606 mg, 2.43 mmol), Colorless solid, mp 49–51 °C. ^{1}H NMR (400 MHz, $CDCl_3$): δ 7.19 (1H, t, J = 8.0 Hz), 7.68 (1H, m), 7.91 (1H, m), 9.99 (1H, d, J = 2.4 Hz).

2-Iodo-5-methoxybenzaldehyde

Yield 98% (642 mg, 2.45 mmol), Colorless solid, mp 113–116 °C. ^{1}H NMR (400 MHz, $CDCl_3$): δ 3.84 (3H, s), 6.92 (1H, dd, J = 8.8 Hz, 3.2 Hz), 7.43 (1H, d, J = 3.2 Hz), 7.80 (1H, d, J = 7.6 Hz), 10.03 (1H, s).

4-Fluoro-2-iodoacetophenone

Yield 98% (647 mg, 2.45 mmol), Colorless solid, mp 45–46 °C. ^{1}H NMR (400 MHz, $CDCl_3$): δ2.59 (3H, t, J = 2.4 Hz), 7.11 (1H, m), 7.52 (1H, m), 7.65 (1H, m).

3-Iodothiophene-2-carboxaldehyde

Yield 99% (589 mg, 2.48 mmol), Colorless solid, mp 82–85 °C. ^{1}H NMR (400 MHz, $CDCl_3$): δ7.28 (1H, d, J = 4.8 Hz), 7.70 (1H, dd, J = 5.2 Hz, 1.2 Hz), 9.83 (1H, d, J = 1.2 Hz).

Typical procedure for the synthesis of aryl(iodo)(4-methylphenyl)bismuthane

To a round-bottomed flask (50 mL) equipped with a magnetic stir bar were added bismuth(III) chloride (422 mg, 1.33 mmol) and tris(4-methylphenyl)bismuthane (323 mg, 0.67 mmol). After dry diethyl ether (6 mL) was added to the flask at room temperature, the mixture was stirred for 1 h. To another round-bottomed flask (50 mL) were added 2′-iodoacetophenone derivative (1 mmol), zinc (262 mg, 4 mmol) and dry DMF (5 mL). The flask was set in an ultrasonic water bath at room temperature (25 °C) and the resulting mixture was sonicated for 1.5–2 h, during which time the water bath temperature rose to 48 °C by itself. The sonication was stopped and unreacted zinc powder precipitated. The resulting supernatant solution containing an arylzinc reagent was slowly transferred to the suspension of dichloro(4-methylphenyl)bismuthane (ca. 2 mmol) thus formed, and the resulting mixture was stirred for 3.5–5 h at room temperature. The reaction was quenched with aqueous solution of NaI (3 mL) and the resulting mixture was extracted with ethyl acetate (3 × 50 mL). The combined extracts were concentrated to leave an oily residue, which was chromatographed on silica gel with hexane–ethyl acetate (5:1) to afford the corresponding iodobismuthane.

(2-Acetylphenyl)iodo(4-methylphenyl)bismuthane 5a

Yellow crystal, Yield 35% (191 mg, 0.35 mmol), mp 160–162 °C. ^{1}H NMR (400 MHz, $CDCl_3$): δ2.25 (3H, s), 2.69 (3H, s), 7.25 (2H, d, J = 6.8 Hz), 7.71 (1H, dt, J = 1.2, 7.6 Hz), 7.88 (1H, dt, J = 1.2, 7.6 Hz), 8.07 (2H, d, J = 8.0 Hz), 8.22 (1H, dd, J = 1.2, 7.6 Hz), 9.41 (1H, dd, J =

0.8, 7.2 Hz). ^{13}C NMR (100 MHz, $CDCl_3$): δ 21.54, 27.08, 128.50, 132.36, 134.51, 138.01, 138.21, 138.98, 143.10, 145.55, 166.78, 172.09, 207.54. IR (KBr): ν 3738, 3037, 1622, 1552, 1276 and 761 cm^{-1}. HRMS (APCI) calcd. for $C_{15}H_{14}BiIO$: $[M-H]^-$ 544.9832. found: 544.9821.

(2-Formylphenyl)iodo(4-methylphenyl)bismuthane 6a

Yellow crystal, Yield 56% (298 mg, 0.56 mmol), mp 143–144 °C. ^{1}H NMR (400 MHz, DMSO-d_6): δ 2.21 (3H, s), 7.30 (2H, d, J = 7.6 Hz), 7.86 (1H, t, J = 7.2 Hz), 7.95 (1H, t, J =7.2 Hz), 8.14 (2H, d, J = 7.6 Hz), 8.44 (1H, d, J = 7.2 Hz), 9.02 (1H, d, J = 7.2 Hz), 10.75 (1H, s). ^{13}C NMR (100 MHz, $CDCl_3$): δ 21.55, 128.65, 132.47, 137.58, 138.23, 138.44, 139.63, 143.66, 146.16, 165.99, 170.92, 199.50. IR (KBr): ν 3058, 2857, 1633, 1572, 1553, 1296 and 1207 cm^{-1}. HRMS (APCI) calcd. for $C_{14}H_{12}BiIO$: $[M+H]^+$ 532.9808. found: 532.9810.

(2-Acetyl-5-fluorophenyl)iodo(4-methylphenyl)bismuthane 9a

Yellow crystal, Yield 28% (158 mg, 0.28 mmol), mp 186–188 °C. ^{1}H NMR (400 MHz, DMSO-d_6): δ 2.19 (3H, s), 2.72 (3H, s), 7.29 (2H, d, J = 7.6 Hz), 7.54 (1H, dt, J = 2.0, 8.4 Hz), 8.11 (2H, d, J = 7.6 Hz), 8.55 (1H, dd, J = 4.8, 8.4 Hz), 8.89 (1H, s). ^{13}C NMR (100 MHz, DMSO-d_6): δ 21.13, 27.48, 115.62 (J = 22.6 Hz), 130.94, 132.08, 137.08, 138.67 (J = 44.0 Hz), 138.80, 140.51, 169.52, 172.12, 207.84. IR (KBr): ν 1620, 1575, 1558, 1358, 1299, 1262 and 1201 cm^{-1}. HRMS (APCI) calcd. for $C_{15}H_{13}BiFIO$: $[M-H]^-$ 562.9730. found: 562.9726.

(2-Formyl-5-fluorophenyl)iodo(4-methylphenyl)bismuthane 10a

Yellow crystal, Yield 29% (195 mg, 0.29 mmol), mp 148–149 °C. ^{1}H NMR (400 MHz, DMSO-d_6): δ 2.21 (3H, s), 7.32 (2H, d, J = 7.6 Hz), 7.61 (1H, dt, J = 2.4, 8.4 Hz), 8.18 (2H, d, J = 7.6 Hz), 8.52 (1H, dd, J = 5.2, 8.0), 8.74 (1H, d, J = 6.4 Hz), 10.74 (1H, s). ^{13}C NMR (100 MHz, DMSO-d_6): δ 21.14, 115.75 (J = 22.7 Hz), 131.83, 132.17, 137.05, 139.01, 140.77, 140.78 (J = 20.6 Hz), 169.19, 171.80, 199.67. IR (KBr): ν 3061, 2875, 1638, 1582, 1561, 1259 and 1204. cm^{-1}. HRMS (APCI) calcd. for $C_{14}H_{11}BiFIO$: $[M-H]^-$ 548.9566. found: 548.9570.

(2-Formyl-4-methoxyphenyl)iodo(4methylphenyl)bismuthane 11

Yellow crystal, Yield 31% (175 mg, 0.31 mmol); mp 146–147 °C; ^{1}H NMR (400 MHz, DMSO-d_6): δ 2.21 (3H, s), 3.87 (3H, s), 7.31 (2H, d, J = 8.0 Hz), 7.48 (1H, dd, J = 2.4, 8.0 Hz), 7.99 (1H, d, J = 2.8 Hz), 8.13 (2H, d, J = 7.6 Hz), 8.78 (1H, d, J = 8.0 Hz), 10.66 (1H, s). ^{13}C NMR (100 MHz, $CDCl_3$): δ 21.73, 55.83, 123.11, 125.85, 132.54, 138.36, 138.47, 145.25, 148.10, 160.42, 161.50, 166.54, 199.29. IR (KBr): ν 3027, 2924, 2862, 1640, 1585, 1552, 1460, 1251 and 1044 cm^{-1}. HRMS (APCI) calcd. for $C_{15}H_{14}BiIO_2$: $[M-H]^-$ 560.9770. found: 560.9770.

(2-Formyl-3-thienyl)iodo(4-methylphenyl)bismuthane 12

Yellow crystal, Yield 53% (287 mg, 0.53 mmol), mp 132–133 °C. ^{1}H NMR (400 MHz, $CDCl_3$): δ 2.28 (3H, s), 7.31 (2H, d, J = 7.6 Hz), 8.04 (1H, d, J = 4.4 Hz), 8.09 (1H, d, J = 4.4 Hz), 8.14 (2H, d, J = 7.6 Hz), 10.11 (1H, s). ^{13}C NMR (100 MHz, $CDCl_3$): δ 21.58, 132.67, 138.50, 138.56, 142.08, 145.66, 148.47, 166.97, 174.32, 186.44. IR (KBr): ν 1586, 1483, 1450, 1397, 1337, 1195, 853 and 794 cm^{-1}. HRMS (APCI) calcd. for $C_{12}H_{10}BiIOS$: $[M+H]^+$ 538.9374. found: 538.9374.

(2-Ethoxycarbonylphenyl)iodo(4-methylphenyl)bismuthane 13

Yellow crystal, Yield 61%, mp 125–126 °C. ^{1}H NMR (400 MHz, $CDCl_3$): δ 1.39 (3H, t, J = 7.2 Hz), 2.26 (3H, s), 4.42 (2H, m), 7.26 (2H, d, J = 7.6 Hz), 7.36 (1H, dt, J = 0.8, 7.6 Hz), 7.84 (1H, dt, J = 1.2, 7.6 Hz), 8.09 (2H, d, J = 8.0 Hz), 8.21 (1H, dd, J = 1.2, 7.6 Hz), 9.42 (1H, d, J = 7.2 Hz). ^{13}C NMR (100 MHz, $CDCl_3$): δ 14.09, 21.54, 63.31, 128.29, 132.28, 132.77, 134.35, 137.95, 138.27, 138.70, 143.83, 166.84, 169.52, 175.85. IR (KBr): ν 2990, 1634, 1573, 1373, 1311, 1005, 785 and 733 cm^{-1}. Anal. Calc. for $C_{16}H_{16}BiIO_2$: C, 33.35; H, 2.80. Found: C, 33.32; H, 3.03.

Qualitative antifungal assay: The yeast *S. cerevisiae* W303-1A (*MAT***a** *ade2-1 can1-100 ura3-1 leu2-3,112 trp1-1 his3-11,15*) was used for the qualitative antifungal assay. Yeast

extract-peptone-dextrose (YPD) plates contained 1% yeast extract, 2% peptone, 2% glucose and 1.2% agar. The cells were inoculated at a concentration of 1.3×10^4 cells/mL in YPD agar medium at 48 °C and YPD plates were immediately made in Petri dishes. Each compound was dissolved in dimethyl sulfoxide (DMSO) at a concentration of 30 mM and 5 μL of each solution was directly spotted on the surface of the plate. The plates were incubated for 24 h at 30 °C and antifungal activity was indicated by the presence of clear inhibition zones around the spot. The control experiment showed that DMSO does not inhibit fungal growth at all. In order to know the error on the inhibition zone, we carried out the antifungal assay of compounds many times and confirmed that the error was within ±1 mm.

DFT calculation of the association energies: The geometries of the bismuth compounds and the corresponding MeS^--adduct anions in Table 3 were fully optimized in water through density functional theory (DFT) calculations within the polarizable continuum model (PCM) using the Gaussian 09 program package.[25] The hybrid B3LYP exchange-correlation functional and 6-31+G*/lanl2dz mixed basis set (lanl2dz effective core potential for bismuth and iodine and 6-31+G* basis set for the remaining atoms) were employed. All d functions in 6-31+G* are pure 5 D basis functions, which is the default form in the Gaussian 09 GenECP calculations. The exothermicity for the nucleophilic addition of MeS^- was calculated from the energies in water of each substrate, in which only the most stable conformer with the lowest energy was considered.

5 REFERENCES

1. X. Chen, Y. Yamamoto, and K.-y. Akiba, *Heteroatom Chem.* **1995**, *6*, 293.
2. K. Ohkata, S. Takemoto, M. Ohnishi, and K.-y. Akiba, *Tetrahedron Lett.* **1989**, *30*, 4841.
3. C. Silvestru, H. J. Breunich, and H. Althaus, *Chem. Rev.* **1999**, *99*, 3277.
4. T. Murafuji, T. Mutoh, K. Satoh, K. Tsunenari, N. Azuma, and H. Suzuki, *Organometallics* **1995**, *14*, 3848.
5. Y. Hong, Y.-T. Lai, G. C.-F. Chan, and H. Sun, *Proc. Natl. Acad. Sci. USA* **2015**, *112*, 3211.
6. D. M. Keogan, and D. M. Griffith, *Molecules* **2014**, *19*, 15258.
7. K. Onishi, M. Douke, T. Nakamura, Y. Ochiai, N. Kakusawa, S. Yasuike, J. Kurita, C. Yamamoto, M. Kawahata, K. Yamaguchi, and T. Yagura, *J. Inorg. Biochem.* **2012**, *117*, 77.
8. I. P. Ferreira, E. D. L. Piló, A. A. Recio-Despaigne, J. G. Da Silva, J. P. Ramos, L. B. Marques, P. H. D. M. Prazeres, J. A. Takahashi, E. M. Souza-Fagundes, W. Rocha, and H. Beraldo, *Bioorg. Med. Chem.* **2016**, *24*, 2988.
9. D. H. A. Ishak, K. K. Ooi, K.-P. Ang, A. M. Akim, Y.-K. Cheah, N. Nordin, S. N. B. A. Halim, H.-L. Seng, and E. R. T. Tiekink, *J. Inorg. Biochem.* **2014**, *130*, 38.
10. M. Li, Y. Lu, M. Yang, Y. Li, L. Zhang, and S. Xie, *Dalton Trans*. **2012**, *41*, 12882.
11. T. Murafuji, M. Tomura, K. Ishiguro, and I. Miyakawa, *Molecules* **2014**, *19*, 11077.
12. T. Murafuji, K. Nishio, M. Nagasue, A. Tanabe, M. Aono, and Y. Sugihara, *Synthesis* **2000**, 1208.
13. M. Urano, S. Wada, and H. Suzuki, *Chem. Commun.* **2003**, 1202.
14. V. Stravila, J. J. Thurston, D. Prietro-Centurion, and K. H. Whitmire, *Organometallics* **2007**, *26*, 6864.
15. K. Urgin, C. Aubé, C. Pichon, M. Pipelier, V. Blot, C. Thobie-Gautier, E. Léonel, D. Dubreuil, and S. Condon, *Tetrahedron Lett.* **2012**, ***53***, 1894.
16. K. Takagi, *Chem. Lett.* **1993**, *22*, 469.

17. H. Takahashi, S. Inagaki, Y. Nishihara, T. Shibata, and K. Takagi, *Org. Lett.* **2006**, *8*, 3037.

18. A. Krasovskiy, V. Malakhov, A. Gavryushin, and P. Knochel, *Angew. Chem. Int. Ed.* **2006**, *45*, 6040.

19. T. Murafuji, Y. Miyoshi, M. Ishibashi, A. F. M. Mustafizur Rahman, Y. Sugihara, I. Miyakawa, and H. Uno, *J. Inorg. Biochem.* **2004**, *98*, 547.

20. T. Murafuji, Y. Fujiwara, D. Yoshimatsu, I. Miyakawa, K. Migita, and Y. Mikata, *Eur. J. Med. Chem.* **2011**, *46*, 519.

21. T. Murafuji, K. Kitagawa, D. Yoshimatsu, K. Kondo, K. Ishiguro, R. Tsunashima, I. Miyakawa, and Y. Mikata, *Eur. J. Med. Chem.* **2013**, *63*, 531.

22. P. Jeschke, *Pest Manag. Sci.* **2010**, *66*, 10.

23. P. Jeschke, *ChemBioChem.* **2004**, *5*, 570.

24. A. F. M. Hafizur Rahman, T. Murafuji, K. Yamashita, M. Narita, I. Miyakawa, Y. Mikata, K. Ishiguro, and S. Kamijo, *Heterocycles* **2018**, *96*, 1037.

25. M. J. Frisch, G. W. Trucks, H. B. Schlegel, G. E. Scuseria, M. A. Robb, J. R. Cheeseman, G. Scalmani, V. Barone, B. Mennucci, and G. A. Petersson, *et al.* Gaussian 09, Revision C.01; Gaussian, Inc.: Wallingford, CT, USA **2010**.

26. N. Burford, M. D. Eelman, D. E. Mahony, and M. Morash, *Chem. Commun.* **2003**, 146.

27. T. Murafuji, M. Nagasue, Y. Tashiro, Y. Sugihara, and N. Azuma, *Organometallics* **2000**, *19*, 1003 and references cited therein.

28. J. Chen, T. Murafuji, and R. Tsunashima, *Organometallics* **2011**, *30*, 4532.

29. H. Suzuki, T. Murafuji, and N. Azuma, *J. Chem. Soc., Perkin Trans. 1* **1992**, 1593.

30. A. Klapars, and S. L. Buchwald, *J. Am. Chem. Soc.* **2002**, *124*, 14844.

SUMMARY

This study can be summarized into the following outlines:

i) **Introduction of the isosteric pyridine ring into the hypervalent bismuth compounds:**

To introduce pyridine bioisosteres into the heterocyclic hypervalent bismuth compounds an efficient synthetic method has been established. Such an establishment gave a good result in enhancing the antifungal activities against the yeast *Saccharomyces cerevisiae* and also an efficient interest to the new hypervalent heterocyclic bismuthanes.

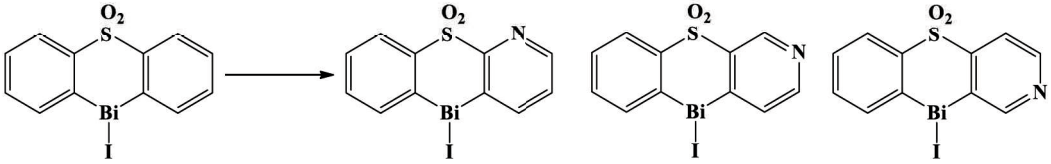

Figure: Replacement of the benzene ring with the pyridine ring

ii) **Functionalization of hypervalent iodobismuthanes by zincation:**

A convenient and effective one-pot method for the synthesis of hypervalent iodobismuthanes functionalized with a carbonyl group has been established by zincation. Furthermore, the DFT calculation of the association energy of the iodobismuthanes have revealed that the acetylazole and acetylthiazole skeletons will carry a fruitful synthetic interest in near future, and zincation is a very effective method for such kinds of synthesis.

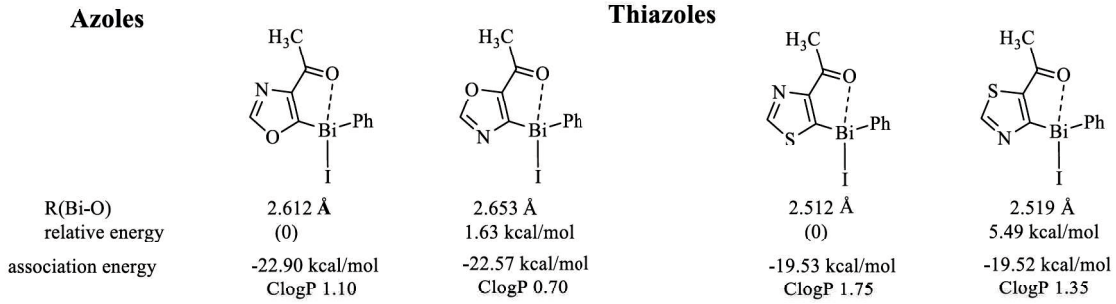

Scheme: Association energy of iodobismuthanes derived from acetylazoles and acetylthiazoles

Acknowledgements

I wish to acknowledge my heartiest regards, richest sense of gratitude and indebtedness to my respected guide **Professor Dr. Toshihiro Murafuji,** Graduate school of Medicine, Yamaguchi University for his direct supervision, personal co-operation, constant guidance, active encouragement and keen interest to carry out this research work.

I am conveying my sincere gratefulness to Associate Professor Dr. Shin Kamijo for his scholastic suggestions, helpful co-operation and continuing inspiration during the period of my research work.

I am enormously grateful to Professor Isamu Miyakawa and Professor Katsuya Ishiguro, Professor Jun Kawamata, Associate Professor Yasutaka Suzuki for their invaluable helps, fruitful suggestions and cordial co-operations during this research course.

It is my pleasant duty to thank Professor Yuji Mikata (Department of Chemistry, Biology, and Environmental Science, Nara Women's University) for the X-ray structure analysis and useful suggestions.

I would like to take the opportunity of thanking to Hiroko Hirata (Secretary, The Japanese society for Time Studies Secretariat) and Professor Kensuke Honda for their valuable suggestions, constant help and encouragement during the study in Japan.

I am also thankful to all the past and present members of the laboratory, especially Kohhei Shintaku, Hiroki Tanaka, Arika Hasegawa, Mayu Oji, Mayu Shirane, Masahiro Narita, Yuya Shimamoto, Manami Sato, Miki Yoshida, Shoya Fujishita, Kiyotaka Maruoka, Haruka Kimura, Saki Yamashita, Junki Sakamoto, Kohhei Nagao, Risa Takai, Hikari Kashou, Toshihiro Yasuda, Hinako Ishibe, Shun Ikeda, Mioto Kosahara and Yuya Tashiro for their helps and active co-operations during the course of my research in this laboratory.

Finally, I am deeply grateful to almighty Allah and also to my parents, family, wife, brother and son for their inspiration of all kinds of supports during the course of my study in Japan.

(A. F. M. Hafizur Rahman)

September, 2018